corresponding to length of n-alkyl side chain (Fig. 2A). Compounds **10** and **11** exhibit EC_{50} values of 2.7 and 5.9 μM, respectively, SI values of 29.6 and 9.80, respectively, and *Clog P* values of 4.90 and 5.96, respectively, suggesting that high hydrophobic property of n-alkyl side chain decreases anti-HCV activity. The appropriate *Clog P* value of caffeic acid ester containing unsaturated side chain may be around 5.

Dihydrocaffeic acid methyl ester (compound **12**) showed less activity than caffeic acid methyl ester (compound **7**) regardless of values of *Clog P* value and CC_{50}, suggesting that the alpha, beta-unsaturated part attached to ester affects the anti-HCV activity level (Table 3 and Figure S3).

We further examined the effect of the hydroxyl groups on the aromatic ring on HCV replication (Table 4 and Figure S4). The EC_{50} values of *O*-methylated caffeic acid n-octyl esters (compounds **13** and **14**) were higher than that of compound **10**. Compounds **15** including 3, 4-di-*O*-methylated caffeic acid n-octyl ester exhibited higher EC_{50} than values of compounds **10**, **13** and **14**. However, addition of a third hydroxyl group to 3, 4, 5-trihydroxy derivative (compound **16**) of compound **10** resulted in a reduction of anti-HCV activity. Furthermore, *Clog P* values of compound **10**, **13**, **14**, **15** and **16** were not correlated with anti-HCV activity (EC_{50} value) (Fig. 2B). These results suggest that the catechol moiety plays an important role in anti-HCV activity, and that the 4-hydroxy moiety is more important for the activity than the 3-hydroxy moiety.

Thus, compound **10**, which exhibits the lowest EC_{50} value and the highest SI value, is the most effective compound among CAPE analogues used in this study.

Effect of CAPE derivatives on virus production

The structure of compound **10** is shown in Fig. 3A. Treatment with compound **10** reduced HCV replication and NS3 protein in a dose-dependent manner at a higher anti-HCV level than

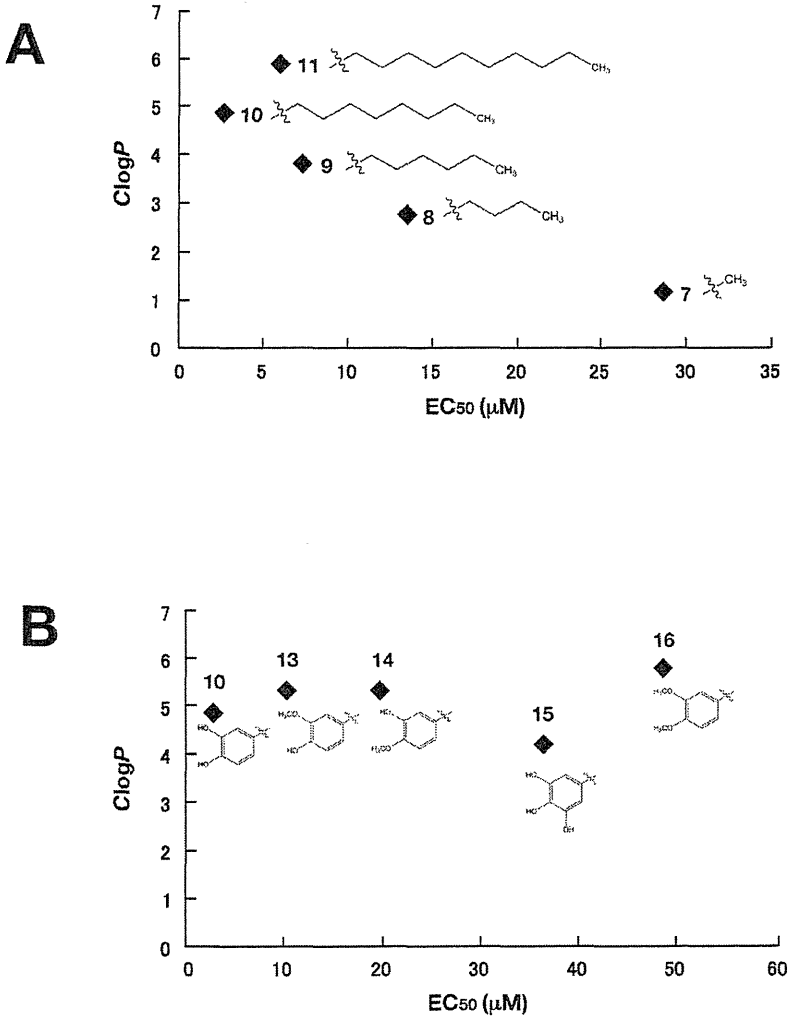

Figure 2. Correlation between the inhibitory effect on HCV replication *and* Clog *P* of CAPE analogues. Values of *x*-axis indicate EC_{50} values of CAPE analogues, while values of *y*-axis show Clog *P* values. (A) Correlation between the inhibitory effect on HCV replication and Clog *P* of CAPE analogues (Compound 7–11). (B) Correlation between the inhibitory effect on HCV replication and Clog *P* of CAPE analogues (Compound 10 and 13–16).
doi:10.1371/journal.pone.0082299.g002

Table 2. Effect of caffeic acid esters **7, 9–14**, including **1**, on HCV replication.

Compound No.	R	EC_{50} [a] (μM)	CC_{50} [b] (μM)	SI [c]	Clog P [d]
7	CH_3	28.6±1.2	122.1±5.0	4.2	1.20
8	C_4H_9	13.5±2.1	39.0±1.1	2.9	2.79
9	C_6H_{13}	7.3±0.2	37.6±1.2	5.1	3.85
10	C_8H_{17}	2.7±0.1	71.7±8.5	26.6	4.90
11	$C_{10}H_{21}$	5.9±0.9	57.9±2.9	9.8	5.96
1	$(CH_2)_2Ph$	9.0±0.7	136.1±1.9	17.9	3.30

The basic structure and side moieties are shown in Figure S2.
a: Fifty percent effective concentration based on the inhibition of HCV replication.
b: Fifty percent cytotoxicity concentration based on the reduction in cell viability.
c: Selectivity index (CC_{50}/EC_{50}).
d: Determined with ChemDraw software (Chem Bio Office Ultra, 2008).
doi:10.1371/journal.pone.0082299.t002

compound **1** (Figs. 3B and C), but not effect enzymatic activities of firefly and *Renilla* luciferases (Fig. 3D) and IRES-dependent translation (Fig. 3E), suggesting that inhibition of HCV replication by compound **10** is not due to offtarget effect. We evaluated the inhibitory effect of compound **10** on three different subgenomic replicon cell lines (1b: N strain, Con1 strain, 2a: JFH-1 strain) and one full genome replicon cell line (1b: O strain). Compound **10** inhibited the viral replication of all replicon cell lines at similar level, and exhibited the lowest EC_{50} value of 1.0 μM and an SI value of 63.1 by using Con1 replicon cells (Table 5). We next examined the effect of compound **10** on virus production by using HCVcc, since subgenomic replicon mimics HCV replication, but not the whole viral cycle. The Huh7 OK1 cell line, which is highly permissive to the HCV JFH1 strain [22], was infected with HCVcc and then treated with compound **10** at 24 h post-infection. The supernatant was harvested 72 h post-infection from the culture supernatant and then the RNA that prepared from the supernatant was estimated by real time qRT-PCR. Figure 3F shows that treatment with compound **10** reduced HCV viral production (EC_{50} = 1.8±0.4 μM) in a similar way to the data obtained by using a replicon cell line. To clarify whether or not compound **10** inhibited HCV replication via interferon-signaling pathway, we analyzed ISRE activity and the expression of interferon stimulated gene (ISG) by using reporter assay and RT-PCR, respectively. The replicon cells were harvested at 48 h post-treatment. There were no significant effects of compound **1**, **6** and **10** on ISRE-promoter activities, while interferon alpha 2b significantly enhanced it as a positive control (Fig.4 A). The data of the RT-PCR analysis showed that the transcriptional expressions of ISGs including Mx1, MxA, IFIT4, ISG15, OAS1, OAS2, and OAS3 were induced with interferon alpha 2b, but not with compound **1**, **6** and **10** (Fig. 4B). These data suggest that the CAPE derivatives have an inhibitory effect on virus production and replication, irrespective of interferon signaling induction.

Synergistic effect of caffeic acid n-octyl ester on interferon and direct-acting antiviral agents

To estimate the effects of drug combinations on anti-HCV activity, we examined the antiviral activity of compound **10** in combination with IFN-α 2b, telaprevir (NS3 protease inhibitor), danoprevir (NS3 protease inhibitor), daclatasvir (NS5A inhibitor) or VX-222 (NS5B polymerase inhibitor). Con1 LUN Sb #26 replicon cells were treated with compound **10** in combination with

Table 3. Effect of caffeic acid esters **7**and **8** on HCV replication.

Compound No.	EC_{50} [a] (μM)	CC_{50} [b] (μM)	SI [c]	Clog P [d]
7	28.6±1.2	122.1±5.0	4.2	1.20
12	77.0±1.6	140.7±3.4	1.8	1.02

Chemical structures of both compounds are shown in Figure S3
a: Fifty percent effective concentration based on the inhibition of HCV replication.
b: Fifty percent cytotoxicity concentration based on the reduction in cell viability.
c: Selectivity index (CC_{50}/EC_{50}).
d: Determined with ChemDraw software (Chem Bio Office Ultra, 2008).
doi:10.1371/journal.pone.0082299.t003

each anti-HCV agent at various concentration rations for 72 h. The effect of each drug combination on HCV replication was analyzed by using CalcuSyn. An explanatory diagram of isobologram was shown at a right end of lower panels of Fig. 5A as described in Materials and Methods. As shown in the resulting isobologram, all plots of the calculated EC_{90} values of compound **10** with IFN-alpha 2b, daclatasvir, or VX-222 are located under the additive line, while the plots of compound **10** with telaprevir, or danoprevir are located above the additive line and closed to the additive line (Fig. 5A). Additionally, we determined the degree of inhibition for each drug combination was analyzed as the combination index (CI) calculation at 50, 75 and 90% of effective concentrations by using CalcuSyn. An explanatory diagram was shown at a right end of lower panels of Fig. 5B as described in Materials and Methods. On the basis of the CalcuSyn analysis, the combination of compound **10** with daclatasvir exhibited strong synergistic effect on inhibition of HCV replication in the replicon cells (Fig. 5B, upper middle). The combination of compound **10** with VX-222 exhibited an additive to synergistic effect, suggesting that it trends toward synergistic (Fig. 5B, upper right), and with IFN-alpha 2b exhibited an antagonistic to synergistic effect, suggesting that it trends toward synergistic (Fig. 5B, upper left). In contrast, the combination of compound **10** with telaprevir resulted in antagonistic effect (Fig. 5B, lower left), and with danoprevir resulted in an antagonistic to additive effect, suggesting it trends toward antagonistic (Fig. 5B, lower middle). These calculated data

Table 4. Effect of octyl esters **10** and **13–16** on HCV replication.

Compound No.	R^1, R^2, R^3	EC_{50} [a] (μM)	CC_{50} [b] (μM)	SI [c]	Clog P [d]
10	$R^1=R^2=R^3=H$	2.7±0.1	71.7±8.5	26.6	4.90
13	$R^1=CH_3$, $R^2=R^3=H$	10.2±1.1	60.3±1.6	5.9	5.35
14	$R^1=R^3=H$, $R^2=CH_3$	19.6±0.8	59.2±1.4	3	5.35
15	$R^1=R^2=CH_3$, $R^3=H$	48.5±1.7	212.4±6.9	4.4	5.82
16	$R^1=R^2=H$, $R^3=OH$	36.3±2.9	59.8±6.9	1.6	4.24

The basic structure and side moieties are shown in Figure S4.
a: Fifty percent effective concentration based on the inhibition of HCV replication.
b: Fifty percent cytotoxicity concentration based on the reduction in cell viability.
c: Selectivity index (CC_{50}/EC_{50}).
d: Determined with ChemDraw software (Chem Bio Office Ultra, 2008).
doi:10.1371/journal.pone.0082299.t004

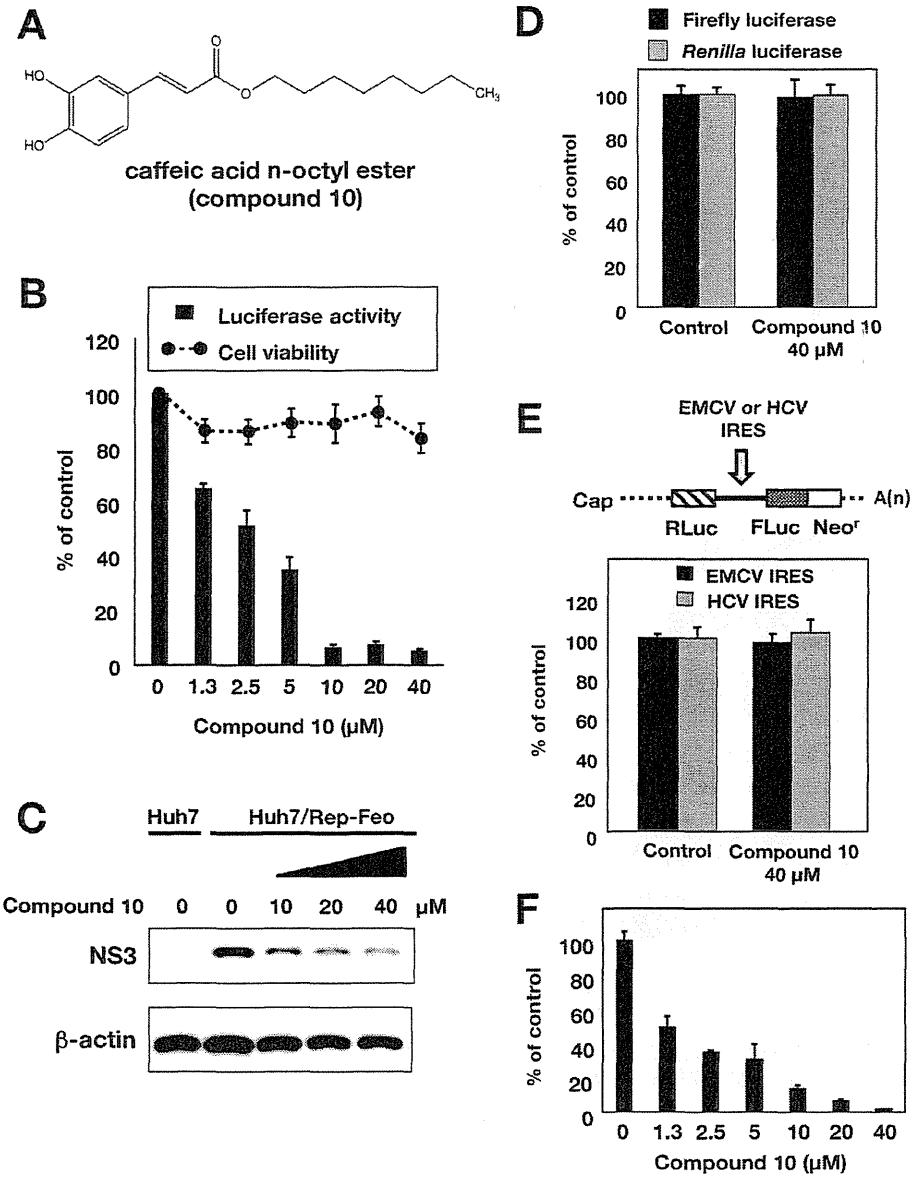

Figure 3. Effect of compound 10 on the viral replication in the replicon cell line and HCVcc. (A) Molecular structure of compound **10**. (B) Huh7/Rep-Feo cells were incubated for 72 h in a medium containing various concentrations of compound **10**. Luciferase and cytotoxicity assays were carried out by the method described in Materials and Methods. Error bars indicate standard deviation. The data represent three independent experiments. (C) Protein extract was prepared from Huh7/Rep-Feo cells treated for 72 h with the indicated concentration of compound **10** and it was then subjected to Western blotting using antibodies to NS3 and beta-actin. (D) Huh7 cell line was transfected with pEF Fluc IN encoding firefly luciferase or pEF Rluc IN encoding *Renilla* luciferase. Both transfected cell lines were incubated with DMSO (Control) or 40 μg/ml compound **10**. Firefly or *Renilla* luciferase activity was measured 72 h post-treatment. Luciferase activity was normalized with protein concentration. Error bars indicate standard deviation. The data were represented from three independent experiments. (E) Schematic structure of RNA transcribed from the plasmids was shown (Top). The bicistronic gene is transcribed under the control of elongation factor 1α (EF1α) promoter. The upstream cistron encoding *Renilla* luciferase (RLuc) is translated by a cap-dependent mechanism. The downstream cistron encodes the fusion protein (Feo), which consists of the firefly luciferase (Fluc) and neomycin phosphotransferase (Neo^r), and is translated under the control of the EMCV or HCV IRES. Huh7 cell line was transfected with each plasmid and incubated for 72 h post-treatment with DMSO (control) or 40 μg/ml of compound **10**. Firefly and *Renilla* luciferase activities were measured. Relative ratio of Firefly luciferase activity to *Renilla* luciferase activity was represented as percentage of the control condition. Error bars indicate standard deviation. The data were represented from three independent experiments. (F) Huh7 OK1 cell line was infected with HCVcc derived from JFH-1 strain and then treated with several concentrations of compound **10** at 24 h post-infection. The resulting cells were harvested 72 h post-infection. The viral RNA of supernatant was purified and estimated by the method described in Materials and Methods. Error bars indicate standard deviation. The data represent three independent experiments. Treatment with DMSO corresponds to '0'.
doi:10.1371/journal.pone.0082299.g003

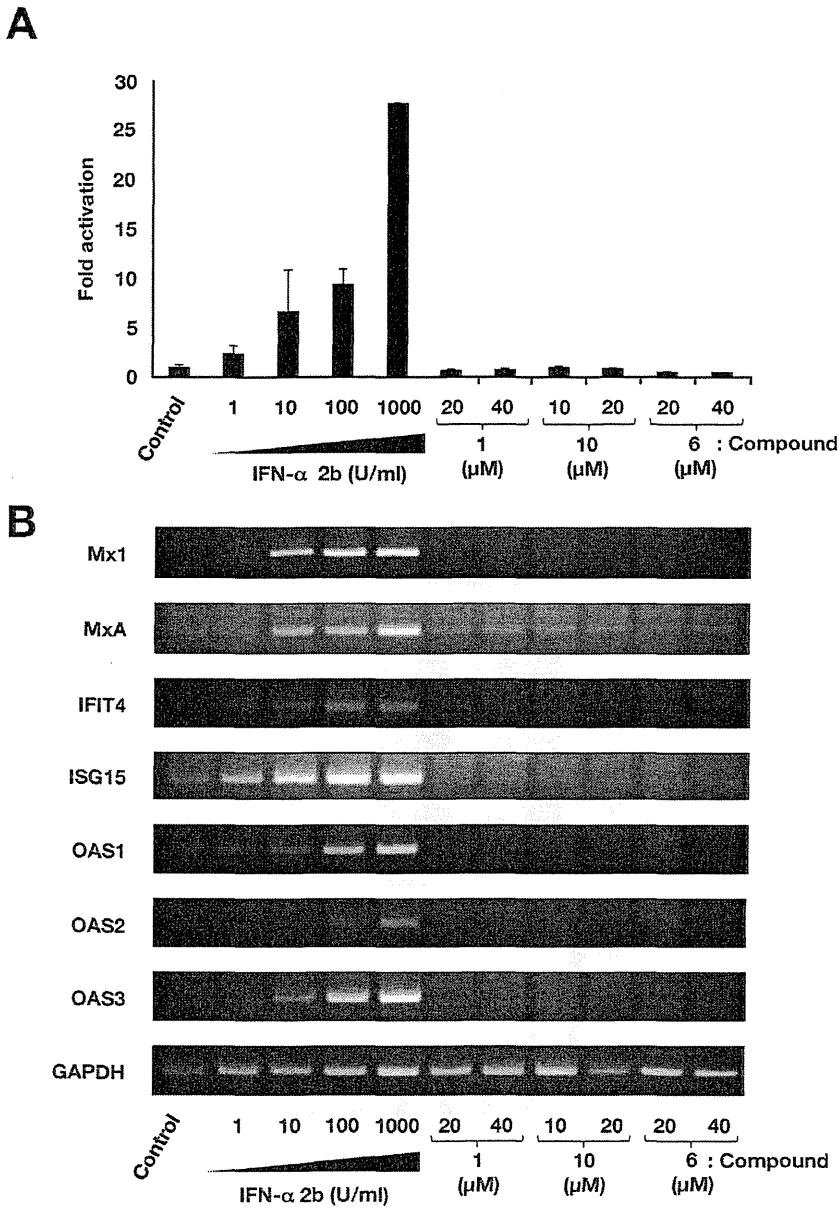

Figure 4. Effect of CAPE derivatives on the interferon-signaling pathway. (A) Plasmids pISRE-TA-Luc and phRG-TK were co-transfect into Huh7 OK1 cells. The transfected cells were cultured with 1, 10, 100, or 1000 U/mL of interferon-alpha 2b, and compounds **1**, **6** and **10**. Treatment with DMSO corresponds to '0'. After 48 h of treatment, luciferase activities were measured, and the value were normalized against *Renilla* luciferase activities. Error bars indicate standard deviation. The data represent three independent experiments. (B) Huh7 replicon cell line of genotype 1b was treated with 1, 10, 100, or 1000 U/mL of interferon-alpha 2b, and compounds **1**, **6** and **10** for 48 h. Treatment with DMSO corresponds to the control. The mRNAs of Mx1, MxA, IFIT4, ISG15, OAS1, OAS2, OAS3, and GAPDH as an internal control were detected by RT-PCR.
doi:10.1371/journal.pone.0082299.g004

of combination tests suggest that daclatasvir, IFN-alpha 2b, and VX-222 synergistically, but telaprevir and danoprevir antagonistically, inhibit HCV replication in combination with compound **10**.

Discussion

CAPE is an active component of propolis, which possesses broad-spectrum biological activities [14–19]. In this study, CAPE suppressed HCV RNA replication in a dose-dependent manner (Fig. 1A and B). Treatment with CAPE inhibited HCV replication with an EC_{50} of 9.0 μM and an SI of 17.9 in Huh7/Rep-Feo cells (Table 1). The treatment of the replicon cell line with CAPE did not induce expression of the IFN-inducible gene (Fig. 4), suggesting that the inhibition of HCV replication by CAPE is independent of the IFN signaling pathway.

Table 5. Anti-HCV activity of compound **10** in replicon cell lines of genotypes 1b and 2a.

Cell line	Replicon type	Strain (Genotype)	EC_{50} [a] (μM)	CC_{50} [b] (μM)	SI [c]
Huh7 Rep/Feo-1b	Subgenome	N (1b)	2.7±0.1	71.7±8.5	26.6
Con1 LUN Sb #26	Subgenome	Con1 (1b)	1.0±0.1	63.1±3.1	63.1
Huh7 Rep/Reo-2a	Subgenome	JFH1 (2a)	1.0±0.3	60.0±2.3	60.0
OR6	Full genome	O (1b)	1.5±0.4	61.7±0.6	41.1

a: Fifty percent effective concentration based on the inhibition of HCV replication.
b: Fifty percent cytotoxicity concentration based on the inhibition of HCV replication.
c: Selectivity Index (CC_{50}/EC_{50}).
doi:10.1371/journal.pone.0082299.t005

We also examined the effect of CAPE derivatives on HCV replication. Our data suggest that the n-alkyl side chain and catechol moiety of the CAPE derivative are critical in its anti-HCV activity (Tables 2 and 3). The EC_{50} value of the derivative decreased dependently on the length of the n-alkyl side chain until reaching octyl ester length (Table 2), while longer chains than octyl ester of a derivative led to an increase in the EC_{50} value and *Clog P* value. Compound **10**, Caffeic acid n-octyl ester, exhibited the highest anti-HCV activity among the tested compounds with an EC_{50} value of 2.7 μM and an SI value of 26.6. Cyclosporine A and its analogues could suppress the viral replication of genotype 1b at a higher level than that of genotype 2a [23]. Interestingly, compound **10** could inhibit HCV replication of genotype 1b and 2a at a similar level, irrespective of expression of the interferon-inducible gene (Fig. 4). CAPE and its derivatives may therefore possess a mechanism different from cyclosporine A and its analogues with respect to anti-HCV activity.

CAPE has been reported to be an inhibitor of NF-kappaB [14,20]. Lee et al. reported that the catechol moiety in CAPE was important for inhibition of NF-kappaB activation [24]. The data shown in Table 3 suggest that the catechol moiety in CAPE is critical to the anti-HCV activity of compound **10**. Previous studies have implicated the inhibition of NF-kappaB in anti-HCV activity. Treatment with an extract prepared from *Acacia confusa* [25] or San-Huang-Xie-Xin-Tang [26] could suppress HCV replication and inhibit NF-kappaB activation. However, Chen et al. reported that curcumin-mediated inhibition of NF-kappaB did not contribute to anti-HCV activity [11]. Furthermore, treatment with *N*′-(Morpholine-4carbonyloxy)-2(naphthalene-1-yl) acetimidamide could activate NF-kappaB and downstream gene expression in the same Huh7/Rep-Feo replicon cell line as the cell line used in this study and exhibited potent inhibition of HCV replication without interferon signaling [27]. These reports support the notion that CAPE derivatives do not mainly target NF-kappaB activity as part of their anti-HCV activity.

Several host proteins have been reported to regulate function of NS5A, leading to supporting HCV replication (review in [2,28]). Daclatasvir exhibited potent synergistic effect on anti-HCV activity in combination of compound **10** (Fig. 5). Anti-HCV activity of compound **10** might associate with intrinsic functions of host factors that interact with NS5A. NS3 protease inhibitors exhibited antagonistic effect in combination of compound **10** (Fig. 5). The inhibitory effect of compound **10** might be mediated by the activation of an unknown endogenous protease that is nonspecifically suppressed by NS3 protease inhibitors. Further study to clarify the mechanism by which compound **10** suppresses HCV replication might contribute to identification of a novel host factor as a drug target for development of the effective compound supporting an effect of other anti-HCV drugs.

In conclusion, we showed that CAPE and its analogue possess a significant inhibitory effect against HCV replication. The length of n-alkyl side chains and the catechol moiety of CAPE are critical to its inhibitory activity against HCV replication. The most effective derivative among the tested compounds was caffeic acid n-octyl ester, which exhibited an EC_{50} value of 1 μM and an SI value of 63.1 in the replicon cell line of genotype 1b strain Con1. Treatment with caffeic acid n-octyl ester reduced the viral replication of genotype 1b and 2a at a similar level and inhibited viral production of HCVcc. Treatment with caffeic acid n-octyl ester could synergistically enhance the anti-HCV activities of IFN-α 2b, daclatasvir, and VX-222, but neither telaprevir nor danoprevir. Further investigation to clarify the mechanism of anti-HCV activity and further modification of the compound to improve anti-HCV activity will lead to novel therapeutic strategies to treat chronic hepatitis C virus infection.

Materials and Methods

Compounds

Boldface numbers in this text indicate the compound numbers shown in Tables. All chemical structures of compounds used in this study are shown in figure S1. CAPE (**1**), caffeic acid (**2**), ferulic acid (**3**), and chlorogenic acid (**5**) and were purchased from Sigma-Aldrich (St. Louis, MO, USA). Cinnamic acid phenethyl ester (**4**) was from Tokyo Chemical Industry (Tokyo, Japan). Rosmarinic acid (**6**) was from Wako Pure Chemical (Tokyo, Japan). Caffeic acid n-octyl ester (n-octyl caffeate) (**10**), 3-O-methylcaffeic acid n-octyl ester (n-octyl-3-methylcaffeate) (**13**), 4-O-methylcaffeic acid n-octyl ester (n-octyl-3-methylcaffeate) (**14**), and 3, 4-O-dimethyl-caffeic acid n-octyl ester (n-octyl-3, 4-methylcaffeate) (**15**) were from LKT Laboratories (St. Paul, MN, USA).

Caffeic acid esters **7**, **8**, **9**, and **11** were synthesized by preparing caffeic acid chloride followed by treatment with corresponding alcohols [29]. Dihydrocaffeic acid ester **12** was prepared by hydrogenation of **7**. Compound **16** is a newly synthesized ester. Spectroscopic data of known esters **7–9**, and **11** prepared here were identical to those reported [30-32] Interferon alfa-2b (IFN-α 2b) was obtained from MSD (Tokyo, Japan). Telaprevir and daclatasvir were purchased from Selleckchem (Houston, TX, USA). Danoprevir and VX-222 were from AdooQ BioScience (Irvine, CA, USA).

Chemistry of 3,4,5-Trihydroxycinnamic acid n-octyl ester

3,4,5-Trihydroxycinnamic acid n-octyl ester (**16**) was prepared by condensation of corresponding benzaldehydes with malonic acid n-octyl monoester [33]. A solution of malonic acid n-octyl monoester (432 mg, 2 mmol), 3,4,5-trihydroxybenzaldehyde (462 mg, 3 mmol) and piperidine (0.2 mL) in pyridine (2 mL)

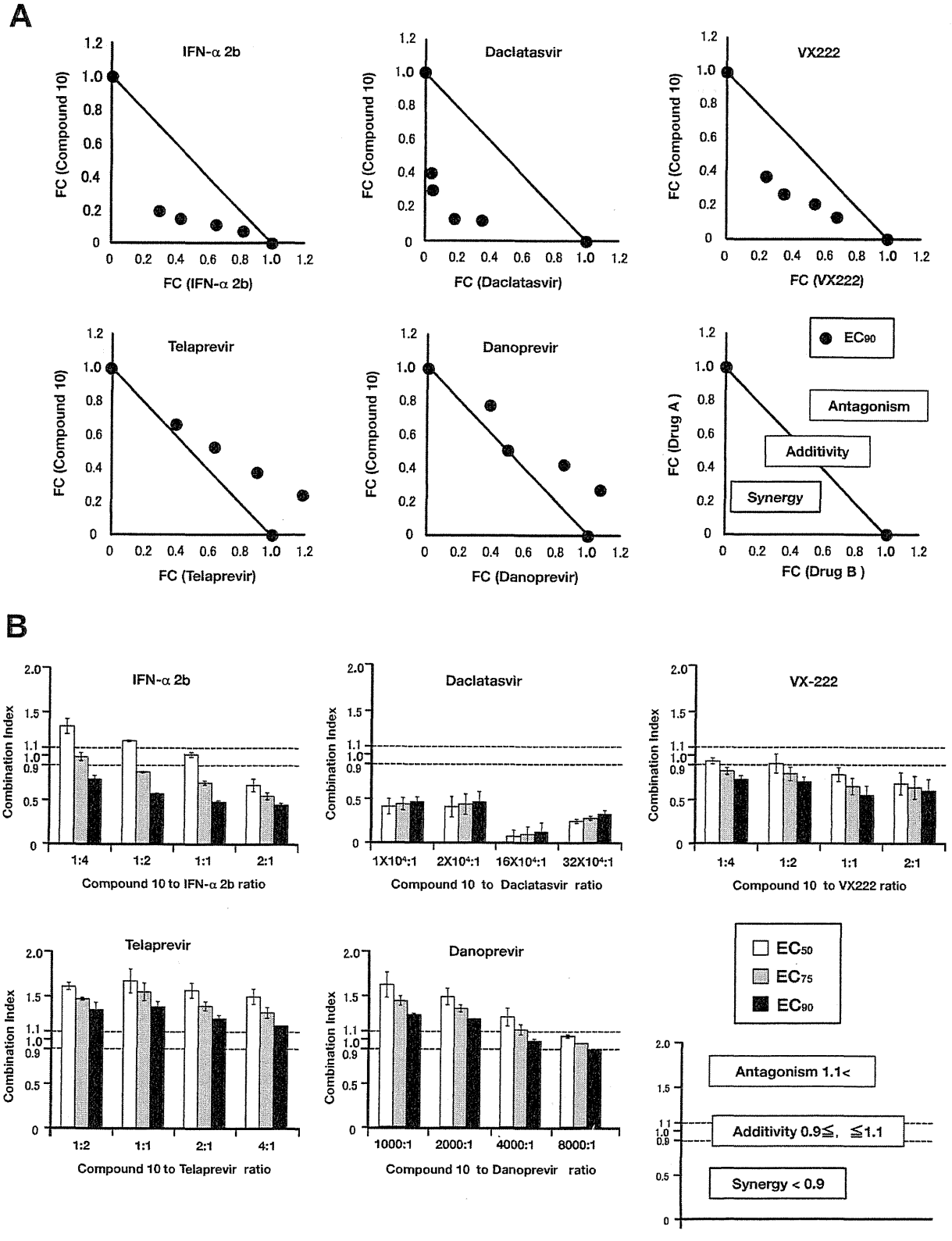
A
IFN-α 2b
FC (Compound 10)
FC (IFN-α 2b)
Daclatasvir
FC (Daclatasvir)
VX222
FC (VX222)
Telaprevir
FC (Telaprevir)
Danoprevir
FC (Danoprevir)
EC90
Antagonism
Additivity
Synergy
FC (Drug A)
FC (Drug B)
B
IFN-α 2b
Combination Index
Compound 10 to IFN-α 2b ratio
Daclatasvir
1X10⁴:1
2X10⁴:1
16X10⁴:1
32X10⁴:1
Compound 10 to Daclatasvir ratio
VX-222
Compound 10 to VX222 ratio
Telaprevir
Compound 10 to Telaprevir ratio
Danoprevir
1000:1
2000:1
4000:1
8000:1
Compound 10 to Danoprevir ratio
EC50
EC75
EC90
Antagonism 1.1<
Additivity 0.9≦, ≦1.1
Synergy < 0.9

Figure 5. Synergistic effect analyses for the combination of compound 10 with IFN-α 2b, daclatasvir, VX-222, telaprevir, or danoprevir. The Huh7 cell line, including the subgenomic replicon RNA of genotype 1b strain Con1, was treated for 72h with combinations of compound 10 and IFN-α 2b, daclatasvir, VX-222, telaprevir, or danoprevir. Luciferase assay were carried out as described in Materials and Methods. (A) The calculated EC_{90} values for combination were plotted as the fractional concentration (FC) of compound 10 and one of IFN-α 2b, daclatasvir, VX-222, telaprevir, and danoprevir on the *x* and *y* axes, respectively. Synergy, antagonism and additivity are indicated in a representative graph as a right end of lower graphs and are described in Materials and Methods. (B) Combination indexes of compound 10 with IFN-α 2b, daclatasvir, VX-222, telaprevir, or danoprevir at the EC50, EC75, and EC90 values were measured at various drug rations. Synergy, antagonism and additivity are indicated in a representative graph as a right end of lower graphs and are described in Materials and Methods.
doi:10.1371/journal.pone.0082299.g005

was heated at 70°C for 1 h. The reaction mixture was concentrated under a vacuum to give a residue, which was dissolved in $CHCl_3$-IPA (3:1, v/v) and then washed with 10% HCl and water. The organic layer was dried over Na_2SO_4 and evaporated to give a residue, which was purified by silica gel column chromatography using AcOEt-hexane (1:1, v/v) as eluent to give the corresponding n-octyl ester (85 mg, 13.8%) as a pale powder. FT-IR vmax (KBr): 3389, 3239, 2923, 1675, 1627, 1606 cm^{-1}. ^1H NMR (400MHz, CD_3OD) δ: 0.86 (3H, t, J = 7.2 Hz), 1.20–1.40 (10H, m), 1.65 (2H, quintet, J = 6.4 Hz), 4.11, (2H, t, J = 6.4 Hz), 6.16 (2H, d, J = 15.6 Hz), 6.55 (2H, s), 7.40 (2H, d, J = 15.6 Hz). 13C NMR (100 Hz, CD_3OD) δ: 14.4, 23.7, 27.1, 29.8, 30.3, 30.4, 32.9, 65.6, 108.5, 115.3, 126.6, 137.5, 147.1, 169.4. CI MS *m/z*: 309 (M^++H). High-resolution CI MS calcd. for $C_{17}H_{25}O_5$ (M^++H) for 309.1702. Found: 309.1686.

Replicon cell lines and virus infection

The Huh7/Rep-Feo cell line, which harbors the subgenomic replicon RNA composed of HCV IRES, the gene of the fusion protein consisting of neomycin phosphotransferase and firefly luciferase, EMCV IRES and a nonstructural gene of genotype 1b strain N in order in Huh7 cell line, was previously established [34]. Thus, the luciferase activity corresponds to the level of HCV RNA replication. The cell line was maintained in Dulbecco's modified Eagle medium containing 10% fetal calf serum and 0.5 mg/mL G418 and cultured in absence of G418 when they were treated with compounds. The Lunet/Con1LUN Sb #26 cell line, which harbors the subgenomic replicon RNA of the Con1 strain (genotype 1b), was described previously [35]. The OR6 cell line, which harbors the full genomic replicon RNA of the O strain (genotype 1b), was described previously [36]. The HCV replicon cell line derived from the genotype 2a strain JFH1 was described previously [37]. The viral RNA derived from the plasmid pJFH1 was transcribed and introduced into Huh7OK1 cells according to the method of Wakita et al. [38]. The virus was amplified by the several times passages. The cells were infected with the virus at a multiplicity of infection (moi) of 1 and then treated with each compound at 24 h post-infection. The culture supernatants were harvested 72 h post-treatment to estimate the viral RNA as described below.

Determination of luciferase activity in HCV replicon cells

The replicon cells were seeded at 2×10^4 cells per well in a 48-well plate 24 h before treatment. Compounds were added to the culture medium to give various concentrations. The resulting cells were harvested 72 h post-treatment and lysed with cell culture lysis reagent (Promega, Madison, WI). The luciferase activity of each cell lysate was estimated using a luciferase assay system (Promega). The resulting luminescence was detected by a Luminescencer-JNR AB-2100 (ATTO, Tokyo, Japan).

Determination of Cytotoxicity in HCV replicon cells

The replicon cells were seeded at a density of 1×10^4 cells per well in a 96-well plate and then incubated at 37°C for 24 h. Compounds were added to the culture medium to give various concentrations and were then harvested 72 h post-treatment. Cell viability was measured using a dimethylthiazol carboxymethoxyphenylsulfophenyl tetrazolium (MTS) assay with a CellTiter 96 aqueous one-solution cell proliferation assay kit (Promega).

Western Blotting

Western blotting was carried out by the method described previously [39]. The antibodies to NS3 (clone 8G-2, mousemonoclonal, Abcam, Cambridge, UK), and beta-actin were purchased from Cell Signaling Technology (rabbit polyclonal, Danvers, MA, USA) and were used as the primary antibodies in this study.

RNA analysis

Total RNAs were prepared from cells by using the RNAqueous-4PCR kit (Life Technologies, Carlsbad, CA). Viral RNA were prepared from culture supernatants by using the QIAamp Viral RNA mini kit (QIAGEN, Hilden, Germany). The viral RNA genome was estimated by the qRT-PCR method described previously [40]. RT-PCR was carried out by the method described previously [41] which was slightly modified at the PCR step. The PCR samples were incubated once for 10 min at 95°C for an initial activation step of the AmpliTaq Gold DNA Polymerase (Life Technologies), and then subjected to an amplification step of 30 repeats of the cycle consisting of three segments as follow: 0.5 min at 95°C, 1 min at 55°C and 1 min at 72°C. The primers used in this study were as follows: Mx1: 5′-AGCCACTGGACTGACGACTT-3′ and 5′-GAGGGCTGAAAATCCCTTTC-3′;

MxA: 5′-GTCAGGAGTTGCCCTTCCCA-3′ and 5′-ATTCCCATTCCTTCCCCGG-3′;

IFIT4: 5′-CCCTTCAGGCATAGGCAGTA-3′ and 5′-CTCCTACCCGTCACAACCAC -3′; ISG15: 5′-CGCAGATCACCCAGAAGAT-3′ and 5′-GCCCTTGTTATTCCTCACCA-3′;

OAS1: 5′-CAAGCTCAAGAGCCTCATCC-3′ and 5′-TGGGCTGTGTTGAAATGTGT-3′;

OAS2: 5′-ACAGCTGAAAGCCTTTTGGA-3′ and 5′-GCATTAAAGGCAGGAAGCAC-3′;

OAS3: 5′-CACTGACATCCCAGACGATG-3′ and 5′-GATCAGGCTCTTCAGCTTGGC-3′;

GAPDH: 5′-GAAGGTGAAGGTCGGAGTC and 5′- GAAGATGGTGATGGGATTTC-3′

Effects on activities of internal ribosome entry site (IRES) and luciferases

Huh7 OK1 cells were transfected with pEF.Rluc.HCV.IRES.-Feo or pEF.Rluc.EMCV.IRES.Feo [39]. These transfected cells were seeded at 2×10^4 cells per well in a 48-well plate 24 h before treatment, treated with DMSO or compound **10**, and then harvested at 72 h post-treatment. The firefly luciferase activities were measured with a luciferase assay system (Promega). The total protein concentration was measured using the BCA Protein Assay Reagent Kit (Thermo Scientific, Rockford, IL, USA) to normalize

luciferase activity. To evaluate the interferon response, Huh7OK1 cells were seeded on a 48 well plate at a density of 2×10^4 cells per well, and transfected with pISRE-TA-Luc (Takara bio, Shiga, Japan) and phRG-TK (Promega). These transfected cells were incubated in the presence of compounds, IFN-α 2b, or DMSO, and then harvested at 48 h post-treatment. The firefly luciferase and *Renilla* luciferase activities were quantified by using Dual luciferase reporter assay system (Promega).

Prediction of ClogP for compounds

The *ClogP* value deduced from chemical structure roughly corresponds to a value of hydrophobicity. The *ClogP* values of compounds used in this study were calculated using the computer software Chem Bio Office Ultra 2008 (PerkinElmer, Cambridge, MA, USA).

Synergistic effect of caffeic acid n-octyl ester on anti-HCV activities of other drugs

The effects of drug-drug combinations were evaluated by using the Con1 LUN Sb #26 replicon cells, and were analyzed by using the computer software CalcuSyn (Biosoft, Cambridge, United Kingdom). Dose inhibition curves of two different drugs were plotted with each other. In each drug combination, EC_{90} values of several combinations of two different drugs were plotted as the fractional concentration (FC) of both drugs on the *x* and *y*-axes. Additivity indicates the line linked between 1.0 FC value points of both drugs in the absence of each other. Synergy and antagonism are indicated by values plotted under and above, respectively, an additivity line. The explanatory diagram of isobologram is shown in a right end of lower panels of Figure 5A. Combination indexes (CIs) were calculated at the EC_{50}, EC_{75}, and EC_{90} by using CalcuSyn. A CI value of less than 0.9 indicates synergy. A CI value ranging from 0.9 to 1.1 indicates additivity. A CI value of more than 1.1 indicates antagonism. The explanatory diagram was shown in a right end of lower panels of Figure 5B.

Supporting Information

Figure S1 Molecular structure of CAPE and commercial CAPE-related compounds. CAPE structure is divided into three parts: (I) the catechol moiety, (II) the alkenyl moiety on alpha, beta -unsaturated ester, and (III) the ester part. Molecular structures of CAPE and its commercial derivatives are shown.
(TIF)

Figure S2 The basic structure and side moieties of compounds shown in Table 2. Each compound structure is represented on the basis of the basic structure (top).
(TIF)

Figure S3 The molecular structures of compounds 7 and 12, which are shown in Table 3. Both compounds are different in alpha, beta-unsaturated or saturated part attached to ester.
(TIF)

Figure S4 The basic structure and side moieties of compounds shown in Table 4. Each compound structure is represented on the basis of the basic structure (top).
(TIF)

Acknowledgments

We thank T. Wakita for kindly providing a plasmid.

Author Contributions

Conceived and designed the experiments: MT KM. Performed the experiments: H. Shen AY MN HY MS H. Shindo SM. Analyzed the data: HK TT NE. Contributed reagents/materials/analysis tools: YF MI NK NS. Wrote the paper: H. Shen AY MT KM.

References

1. Baldo V, Baldovin T, Trivello R, Floreani A (2008) Epidemiology of HCV infection. Curr Pharm Des 14: 1646–1654.
2. Moriishi K, Matsuura Y (2012) Exploitation of lipid components by viral and host proteins for hepatitis C virus infection. Front Microbiol 3: 54.
3. Hijikata M, Kato N, Ootsuyama Y, Nakagawa M, Shimotohno K (1991) Gene mapping of the putative structural region of the hepatitis C virus genome by in vitro processing analysis. Proc Natl Acad Sci USA 88: 5547–5551.
4. Lohmann V, Korner F, Koch J, Herian U, Theilmann L, et al. (1999) Replication of subgenomic hepatitis C virus RNAs in a hepatoma cell line. Science 285: 110–113.
5. Hofmann WP, Zeuzem S (2011) A new standard of care for the treatment of chronic HCV infection. Nat Rev Gastroenterol Hepatol 8: 257–264.
6. Jacobson IM, McHutchison JG, Dusheiko G, Di Bisceglie AM, Reddy KR, et al. (2011) Telaprevir for previously untreated chronic hepatitis C virus infection. N Engl J Med 364: 2405–2416.
7. Sarrazin C, Hezode C, Zeuzem S, Pawlotsky JM (2012) Antiviral strategies in hepatitis C virus infection. J Hepatol 56 Suppl 1: S88–100.
8. Kieffer TL, Kwong AD, Picchio GR (2010) Viral resistance to specifically targeted antiviral therapies for hepatitis C (STAT-Cs). J Antimicrob Chemother 65: 202–212.
9. Ahmed-Belkacem A, Ahnou N, Barbotte L, Wychowski C, Pallier C, et al. (2010) Silibinin and related compounds are direct inhibitors of hepatitis C virus RNA-dependent RNA polymerase. Gastroenterology 138: 1112–1122.
10. Calland N, Albecka A, Belouzard S, Wychowski C, Duverlie G, et al. (2012) (-)-Epigallocatechin-3-gallate is a new inhibitor of hepatitis C virus entry. Hepatology 55: 720–729.
11. Chen MH, Lee MY, Chuang JJ, Li YZ, Ning ST, et al. (2012) Curcumin inhibits HCV replication by induction of heme oxygenase-1 and suppression of AKT. Int J Mol Med 30: 1021–1028.
12. Bachmetov L, Gal-Tanamy M, Shapira A, Vorobeychik M, Giterman-Galam T, et al. (2012) Suppression of hepatitis C virus by the flavonoid quercetin is mediated by inhibition of NS3 protease activity. J Viral Hepat 19: e81–88.
13. Takeshita M, Ishida Y, Akamatsu E, Ohmori Y, Sudoh M, et al. (2009) Proanthocyanidin from blueberry leaves suppresses expression of subgenomic hepatitis C virus RNA. J Biol Chem 284: 21165–21176.
14. Toyoda T, Tsukamoto T, Takasu S, Shi L, Hirano N, et al. (2009) Anti-inflammatory effects of caffeic acid phenethyl ester (CAPE), a nuclear factor-kappaB inhibitor, on Helicobacter pylori-induced gastritis in Mongolian gerbils. Int J Cancer 125: 1786–1795.
15. Ho CC, Lin SS, Chou MY, Chen FL, Hu CC, et al. (2005) Effects of CAPE-like compounds on HIV replication in vitro and modulation of cytokines in vivo. J Antimicrob Chemother 56: 372–379.
16. Chiao C, Carothers AM, Grunberger D, Solomon G, Preston GA, et al. (1995) Apoptosis and altered redox state induced by caffeic acid phenethyl ester (CAPE) in transformed rat fibroblast cells. Cancer Res 55: 3576–3583.
17. Boudreau LH, Maillet J, LeBlanc LM, Jean-Francois J, Touaibia M, et al. (2012) Caffeic acid phenethyl ester and its amide analogue are potent inhibitors of leukotriene biosynthesis in human polymorphonuclear leukocytes. PLoS One 7: e31833.
18. Lee KW, Chun KS, Lee JS, Kang KS, Surh YJ, et al. (2004) Inhibition of cyclooxygenase-2 expression and restoration of gap junction intercellular communication in H-ras-transformed rat liver epithelial cells by caffeic acid phenethyl ester. Ann N Y Acad Sci 1030: 501–507.
19. Fesen MR, Kohn KW, Leteurtre F, Pommier Y (1993) Inhibitors of human immunodeficiency virus integrase. Proc Natl Acad Sci U S A 90: 2399–2403.
20. Natarajan K, Singh S, Burke TR Jr, Grunberger D, Aggarwal BB (1996) Caffeic acid phenethyl ester is a potent and specific inhibitor of activation of nuclear transcription factor NF-kappa B. Proc Natl Acad Sci U S A 93: 9090–9095.
21. Li Y, Zhang T, Douglas SD, Lai JP, Xiao WD, et al. (2003) Morphine enhances hepatitis C virus (HCV) replicon expression. Am J Pathol 163: 1167–1175.
22. Okamoto T, Omori H, Kaname Y, Abe T, Nishimura Y, et al. (2008) A single-amino-acid mutation in hepatitis C virus NS5A disrupting FKBP8 interaction impairs viral replication. J Virol 82: 3480–3489.
23. Ishii N, Watashi K, Hishiki T, Goto K, Inoue D, et al. (2006) Diverse effects of cyclosporine on hepatitis C virus strain replication. J Virol 80: 4510–4520.

24. Lee Y, Shin DH, Kim JH, Hong S, Choi D, et al. (2010) Caffeic acid phenethyl ester-mediated Nrf2 activation and IkappaB kinase inhibition are involved in NFkappaB inhibitory effect: structural analysis for NFkappaB inhibition. Eur J Pharmacol 643: 21–28.
25. Lee JC, Chen WC, Wu SF, Tseng CK, Chiou CY, et al. (2011) Anti-hepatitis C virus activity of Acacia confusa extract via suppressing cyclooxygenase-2. Antiviral Res 89: 35–42.
26. Lee JC, Tseng CK, Wu SF, Chang FR, Chiu CC, et al. (2011) San-Huang-Xie-Xin-Tang extract suppresses hepatitis C virus replication and virus-induced cyclooxygenase-2 expression. J Viral Hepat 18: e315–324.
27. Kusano-Kitazume A, Sakamoto N, Okuno Y, Sekine-Osajima Y, Nakagawa M, et al. (2012) Identification of novel N-(morpholine-4-carbonyloxy) amidine compounds as potent inhibitors against hepatitis C virus replication. Antimicrob Agents Chemother 56: 1315–1323.
28. Moradpour D, Penin F, Rice CM (2007) Replication of hepatitis C virus. Nat Rev Microbiol 5: 453–463.
29. Lee YJ, Liao PH, Chen WK, Yang CY (2000) Preferential cytotoxicity of caffeic acid phenethyl ester analogues on oral cancer cells. Cancer Lett 153: 51–56.
30. Bourne GT, Golding SW, McGeary RP, Meutermans WD, Jones A, et al. (2001) The development and application of a novel safety-catch linker for BOC-based assembly of libraries of cyclic peptides. J Org Chem 66: 7706–7713.
31. Nagaoka T, Banskota AH, Tezuka Y, Saiki I, Kadota S (2002) Selective antiproliferative activity of caffeic acid phenethyl ester analogues on highly liver-metastatic murine colon 26-L5 carcinoma cell line. Bioorg Med Chem 10: 3351–3359.
32. Uwai K, Osanai Y, Imaizumi T, Kanno S, Takeshita M, et al. (2008) Inhibitory effect of the alkyl side chain of caffeic acid analogues on lipopolysaccharide-induced nitric oxide production in RAW264.7 macrophages. Bioorg Med Chem 16: 7795–7803.
33. Zhang Z, Xiao B, Chen Q, Lian XY (2010) Synthesis and biological evaluation of caffeic acid 3,4-dihydroxyphenethyl ester. J Nat Prod 73: 252–254.
34. Yokota T, Sakamoto N, Enomoto N, Tanabe Y, Miyagishi M, et al. (2003) Inhibition of intracellular hepatitis C virus replication by synthetic and vector-derived small interfering RNAs. EMBO Rep 4: 602–608.
35. Frese M, Barth K, Kaul A, Lohmann V, Schwarzle V, et al. (2003) Hepatitis C virus RNA replication is resistant to tumour necrosis factor-alpha. Journal of General Virology 84: 1253–1259.
36. Ikeda M, Abe K, Dansako H, Nakamura T, Naka K, et al. (2005) Efficient replication of a full-length hepatitis C virus genome, strain O, in cell culture, and development of a luciferase reporter system. Biochem Biophys Res Commun 329: 1350–1359.
37. Nishimura-Sakurai Y, Sakamoto N, Mogushi K, Nagaie S, Nakagawa M, et al. (2010) Comparison of HCV-associated gene expression and cell signaling pathways in cells with or without HCV replicon and in replicon-cured cells. J Gastroenterol 45: 523–536.
38. Wakita T, Pietschmann T, Kato T, Date T, Miyamoto M, et al. (2005) Production of infectious hepatitis C virus in tissue culture from a cloned viral genome. Nat Med 11: 791–796.
39. Yamashita A, Salam KA, Furuta A, Matsuda Y, Fujita O, et al. (2012) Inhibition of hepatitis C virus replication and NS3 helicase by the extract of the feather star *Alloeocomatella polycladia*. Mar Drugs 10: 744–761.
40. Fujimoto Y, Salam KA, Furuta A, Matsuda Y, Fujita O, et al. (2012) Inhibition of Both Protease and Helicase Activities of Hepatitis C Virus NS3 by an Ethyl Acetate Extract of Marine Sponge Amphimedon sp. PLoS One 7: e48685.
41. Jin H, Yamashita A, Maekawa S, Yang PT, He LM, et al. (2008) Griseofulvin, an oral antifungal agent, suppresses hepatitis C virus replication in vitro. Hepatology Research 38: 909–918.

OPEN ACCESS Freely available online

PLOS ONE

Hypoxia-Inducible Factors Activate CD133 Promoter through ETS Family Transcription Factors

Shunsuke Ohnishi[1]*, Osamu Maehara[2], Koji Nakagawa[2], Ayano Kameya[2], Kanako Otaki[2], Hirotoshi Fujita[2], Ryosuke Higashi[2], Kikuko Takagi[1], Masahiro Asaka[3], Naoya Sakamoto[1], Masanobu Kobayashi[4], Hiroshi Takeda[2]

1 Department of Gastroenterology and Hepatology, Hokkaido University Graduate School of Medicine, Sapporo, Japan, 2 Department of Pathophysiology and Therapeutics, Faculty of Pharmaceutical Sciences, Hokkaido University, Sapporo, Japan, 3 Department of Cancer Preventive Medicine, Hokkaido University Graduate School of Medicine, Sapporo, Japan, 4 Department of Nursing, Health Sciences University of Hokkaido, Ishikari, Japan

Abstract

CD133 is a cellular surface protein that has been reported to be a cancer stem cell marker, and thus it is considered to be a potential target for cancer treatment. However, the mechanism regulating CD133 expression is not yet understood. In this study, we analyzed the activity of five putative promoters (P1–P5) of CD133 in human embryonic kidney (HEK) 293 cells and colon cancer cell line WiDr, and found that the activity of promoters, particularly of P5, is elevated by overexpression of hypoxia-inducible factors (HIF-1α and HIF-2α). Deletion and mutation analysis identified one of the two E-twenty six (ETS) binding sites (EBSs) in the P5 region as being essential for its promoter activity induced by HIF-1α and HIF-2α. In addition, a chromatin imunoprecipitation assay demonstrated that HIF-1α and HIF-2α bind to the proximal P5 promoter at the EBSs. The immunoprecipitation assay showed that HIF-1α physically interacts with Elk1; however, HIF-2α did not bind to Elk1 or ETS1. Furthermore, knockdown of both HIF-1α and HIF-2α resulted in a reduction of CD133 expression in WiDr. Taken together, our results revealed that HIF-1α and HIF-2α activate CD133 promoter through ETS proteins.

Citation: Ohnishi S, Maehara O, Nakagawa K, Kameya A, Otaki K, et al. (2013) Hypoxia-Inducible Factors Activate CD133 Promoter through ETS Family Transcription Factors. PLoS ONE 8(6): e66255. doi:10.1371/journal.pone.0066255

Editor: Kaustubh Datta, University of Nebraska Medical Center, United States of America

Received February 6, 2013; **Accepted** May 2, 2013; **Published** June 20, 2013

Funding: This study was supported by Grant-in-Aid for Scientific Research (C) from Japan Society for the Promotion of Science (JSPS), and by the Yasuda Memorial Foundation. The funders had no role in study design, data collection and analysis, decision to publish, or preparation of the manuscript.

Competing Interests: The authors have declared that no competing interests exist.

* E-mail: sonishi@pop.med.hokudai.ac.jp

Introduction

A growing body of evidence supports the idea that a small fraction of undifferentiated cells are involved in initiating and sustaining tumor growth. Those cells are referred to as cancer stem cells (CSCs) [1], and CD133 is considered to be a CSC markers in tumors of various tissues including the brain [2], prostate [3], liver [4], pancreas [5] and colon [6,7].

CD133 is a cellular surface glycoprotein comprising five transmembrane regions and two glycosylated extracellular loops, and it has a molecular weight of 97–120 kDa [8,9]. It has been reported that CD133 gene transcription is regulated by five alternative promoters: P1, P2, P3, P4, and P5 (Fig. 1A) [10]. Recent studies have shown that the methylation status of CpG sites in P1 and P2 is involved in epigenetic regulation of CD133 in colorectal and glioblastoma tumors [11,12]. However, the mechanisms underlying the regulation of CD133 expression are not fully understood.

Increased expression of hypoxia-inducible factors (HIFs) has been documented in many solid tumors, and high expression levels of HIF-1α are usually linked to poor prognosis in cancer patients, including those with colorectal cancer [13–15]. HIF is a heterodimer of the basic helix-loop-helix/Per-ARNT-Sim (bHLH-PAS) proteins and comprises of an O_2-labile α-subunit and β-subunit, acting together to bind to the DNA at specific locations called hypoxia response elements (HREs) [16]. Of the three types of α-subunits, HIF-1α and HIF-2α have been studied most extensively [17].

CSCs have been considered to be dependent on HIF-1α and HIF-2α for survival and tumor growth [18]. In addition, several lines of evidence suggest that HIFs promote the expansion of CD133-positive glioma cells [19] or expression of CD133 in lung cancer cells [20]; however, how the expression of the CSC marker protein is regulated by HIF-1α and HIF-2α remains largely unknown.

Therefore, we investigated the activity of CD133 promoters after overexpression of HIF-1α and HIF-2α, and identified an E-twenty six (ETS) ETS binding site (EBS) as a target of HIF-1α and HIF-2α. Subsequently, we investigated the binding of HIF-1α and HIF-2α at EBS and whether HIF-1α and HIF-2α regulate the expression of CD133 in colon cancer cells.

Materials and Methods

Cells

HEK 293 cells (provided by the RIKEN BRC through the National Bio-Resource Project of the MEXT, Japan) and the human colon cancer cell line WiDr (provided by Health Science Research Resources Bank, Osaka, Japan) were cultured in Dulbecco's modified Eagle's medium (Wako, Osaka, Japan) supplemented with 10% fetal bovine serum (Invitrogen, Carlsbad, CA), 100 U/ml penicillin and 100 μg/ml streptomycin (Invitro-

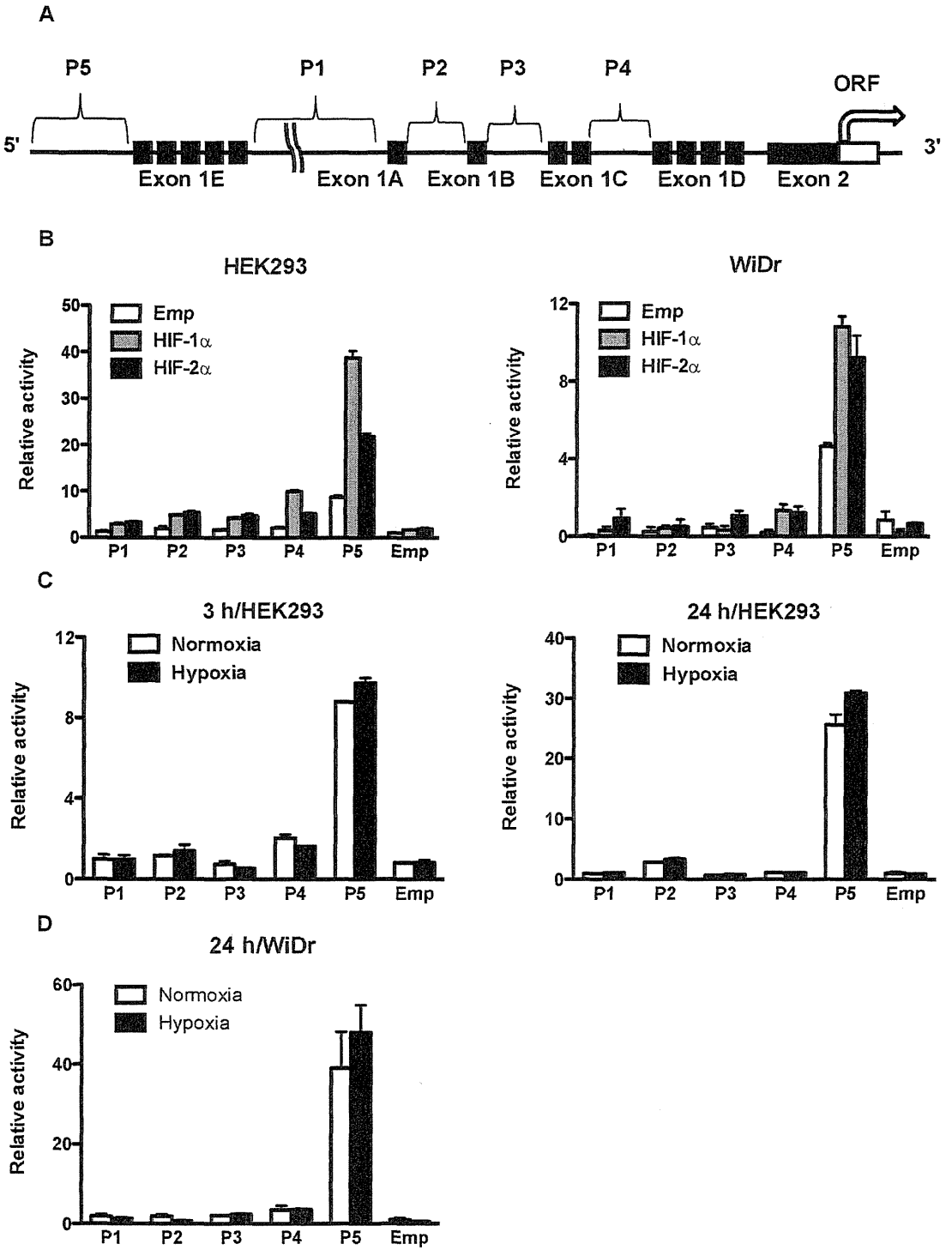

Figure 1. Position of CD133 P5 promoters and their activities after overexpression of HIFs and under hypoxia. (A) Schematic representation of the position of five CD133 promoters (P1–P5) and exon1s (A–E). (B) Promoter activity of P1, P2, P3, P4 and P5 in human embryonic kidney (HEK) 293 cells (left) and human colon cancer WiDr cells (right) after overexpression of HIF-1α and HIF-2α. (C) Promoter activity of P1, P2, P3, P4, and P5 in HEK293 cells under normoxia and hypoxia for 3 hrs (left) and 24 hrs (right). (D) Promoter activity of P1, P2, P3, P4, and P5 in WiDr cells under normoxia and hypoxia for 24 hrs.
doi:10.1371/journal.pone.0066255.g001

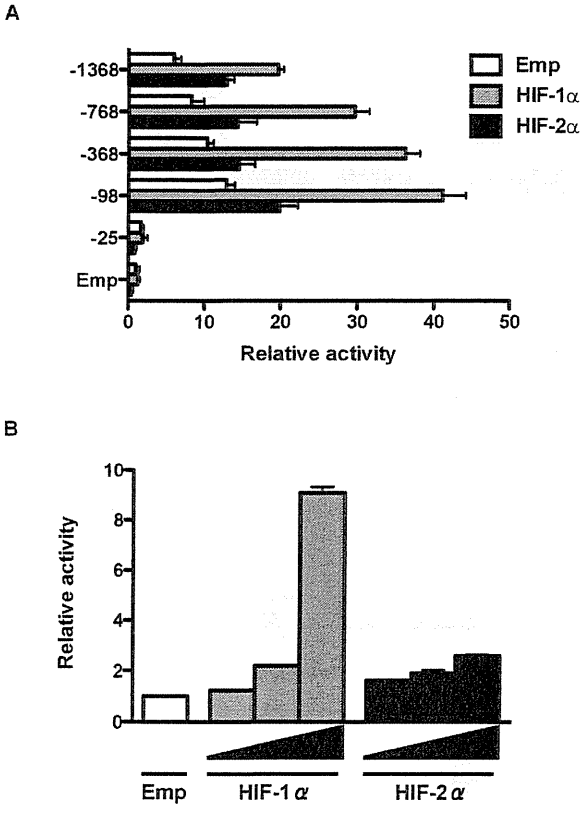

Figure 2. Deletion analysis of CD133 P5 promoter activity and the dose dependent effect of HIFs. (A) Luciferase activities in human embryonic kidney (HEK) 293 cells transfected with a series of deletion mutants of CD133 P5 promoters and HIF-1α or HIF-2α. (B) P5 −98 bp promoter activity of HEK293 cells transfected with a different dose of HIF-1α and HIF-2α.
doi:10.1371/journal.pone.0066255.g002

gen), and incubated at 37°C under normoxia (20% O_2, 5% CO_2) or hypoxia (1% O_2, 5% CO_2).

Plasmids and Small Interfering RNAs (siRNAs)

Complementary cDNAs of HIF-1α, HIF-2α, ETS1 and Elk1 were obtained by RT-PCR and the resulting fragments were cloned into pCMV-3×FLAG and pCI-neo-2×S vectors, which had been constructed by inserting oligonucleotides encoding 3×FLAG and 2×S tag, into pcDNA3.1 vectors (Invitrogen) and pCI-neo (Promega, Madison, WI, USA), respectively. O_2-stable mutants of HIF-1α (P402/564A) and HIF-2α (P405/531A) and dominant negative mutants of ETS1 and Elk1 (ETS1-DN; amino acids 350–485, and Elk1-DN; amino acids 1–168, respectively) were generated using a PCR-based method. The CD133 clones comprising promoter fragments P1–P5-Luc and −1368, −768, −368, −25-Luc of P5 were provided by Dr. S. Tanaka of Hokkaido University, Japan [21]. Mutants of two EBSs (EBS1 and EBS2) in the P5 promoter were constructed, by introducing substitutional mutations into ETS core sequence (GGAA to TTAA), using a PCR-based method. siRNAs for HIF-1α and HIF-2α were purchased from Qiagen (Hilden, Germany).

Transient Transfection and Reporter Gene Assay

Cells were plated at a density of 1×10^5 cells in 24-well plates containing 500 μl of culture medium. After incubation for 24 hrs at 37°C, cells were transfected with 100 ng luciferase plasmid DNA with 10 ng Renilla pGL4.75 (hRluc-CMV) vector (Promega) as an internal control, using lipofectamine2000 (Invitrogen). A reporter gene assay was performed using the Dual Luciferase reporter assay system (Promega), and the luminescence intensity was measured using an AB-2000 Luminescencer-PSN (Atto, Tokyo, Japan) according to the manufacturer's protocol. The transcription activity was normalized according to Renilla luciferase activity. Experiments were performed in triplicates.

Quantitative Real-time Reverse-transcription Polymerase Chain Reaction (qRT-PCR)

Total RNA was extracted from cells using an RNeasy Mini Kit (Qiagen) according to the manufacturer's instructions. RNA was quantified by spectrometry, and the quality was confirmed by gel electrophoresis. One microgram of total RNA was reverse-transcribed into cDNA using an M-MLV reverse transcriptase (Invitrogen). PCR amplification was performed in 50 μl containing 1 μl cDNA and 25 μl Platinum SYBR Green PCR Mix (Invitrogen). β-actin mRNA amplified from the same samples served as an internal control. After an initial denaturation at 95°C for 2 min, a two-step cycle procedure was used (denaturation at 95°C for 15 sec, annealing and extension at 60°C for 1 min) for 40 cycles in a 7700 Sequence Detector (Applied Biosystems). Gene expression levels were determined using the comparative threshold cycle (ddCt) method with β-actin as an endogenous control. The data were analyzed with Sequence Detection Systems software (Applied Biosystems).

Western Blot Analysis

Cells were washed with ice-cold Tris-buffered saline (TBS) (-) and lysed in 1×SDS sample buffer containing 2% 2-mercapto-ethanol. The samples were heated at 95°C for 5 min and then subjected to sodium dodecyl sulfate-polyacrylamide gel electrophoresis (SDS-PAGE). The separated proteins were transferred to Immobilon-P polyvinylidene difluoride (PVDF) membranes (Millipore, Bedford, MA), which were subsequently incubated in TBS with 0.05% Tween 20 (TBST) comprising 5% dried nonfat milk for 30 min at room temperature. Membranes were probed with primary antibodies for HIF-1α (1:250, BD Biosciences, Bedford, MA), HIF-2α (1:200, Santa Cruz Biotechnology, Santa Cruz, CA), CD133 (1:1,000, Cell Signaling, Danvers, MA), and bound antibodies were detected with peroxidase-labeled rabbit or mouse antibodies (Jackson ImmunoResearch Laboratories, West Grove, PA) and visualized using Immobilon Western horse radish peroxidase (HRP) Substrate detection reagents (Millipore).

Chromatin Immunoprecipitation (ChIP) Assay

WiDr cells (1.8×10^6 cells) were plated in 10 cm dish with 10 ml culture medium. After incubation for 24 hrs at 37°C, cells were transfected with 4,000 ng of plasmid encoding FLAG-tagged HIF-1α and HIF-2α. After the incubation period was extended for 48 hrs at 37°C, cells were fixed with 1% formaldehyde and then chromatin was subsequently prepared using the ChIP-IT® Express Kit (Active Motif, Carlsbad, CA) and sheared by sonication. Immunoprecipitation was performed using 15 μg sheared chromatin and 2 μg anti-FLAG antibody (Sigma, St. Louis, MO). DNA collected by ChIP was amplified by qRT-PCR. The target primer was designed for the location of P5 between −98 and +10 (5′-CAGTGTCTCCCCAGAGAG-3′ and 5′-GCAACTTC-

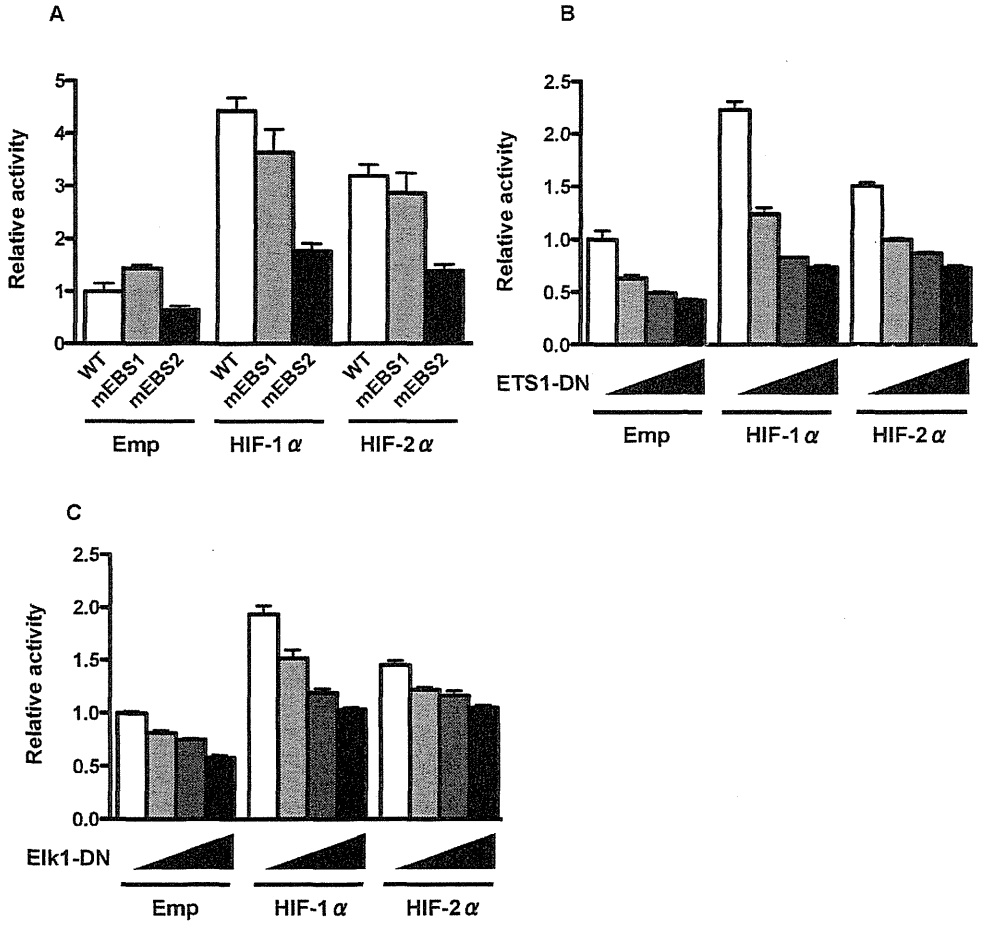

Figure 3. Effect of HIFs and dominant-negative forms of ETS families on the P5 −98 bp promoter. (A) Luciferase activity of the P5 −98 bp promoter with mutation at the two putative EBSs (mEBS1 and mEBS2) after overexpression of HIF-1α or HIF-2α, using human embryonic kidney (HEK) 293 cells. (B, C) Luciferase activity of the P5 −98 bp promoter in HEK293 cells after overexpression of HIF-1α or HIF-2α together with dominant-negative forms of ETS families (ETS1-DN and Elk1-DN).
doi:10.1371/journal.pone.0066255.g003

TACCAGCCTAAGG-3′). For normalization, a control primer was designed at for Exon 2 of CD133 (5′-GGAA-CACGCTTGCCTTCCCCA-3′ and 5′-CCCAGCAGCAA-CAGGGAGCC-3′).

Immunoprecipitation

HEK293 or WiDr cells (5×10^5 cells, respectively) were plated in 6 cm dishes with 6 ml culture medium. After incubation for 24 hrs at 37°C, cells were transfected with 8,000 ng of plasmid DNA (5,000 ng S-tagged HIF-1α or HIF-2α, and 3,000 ng FLAG-tagged ETS transcription factors). After incubation for 48 hrs at 37°C, cells were lysed in 0.4 ml lysis buffer comprising 20 mM Tris–HCl (pH 7.5), 137 mM NaCl, 0.5% NP-40, 0.5 mM dithiothreitol (DTT), complete protease inhibitor cocktail (Roche, Mannheim, Germany), and phosphatase inhibitor cocktail (Sigma), then pre-cleared by centrifuging at 15,000 rpm for 15 min at 4°C. Supernatant was collected as a whole cell lysate. Immunoprecipitation was performed using FLAG M2 agarose (Sigma), and whole cell lysate (360 μl) was added in 10 μl FLAG M2 agarose, then rotated for 1 hr at 4°C. After washing with the lysis buffer, the antigen was eluted using 200 μg/ml 3×FLAG peptide (Sigma) in TBS, then pre-cleared by centrifuging at 5,000 rpm for 2 min at 4°C. 5×SDS sample buffer containing 10% 2-mercaptoethanol was added to the collected supernatant and defined as a loading sample. These samples were analyzed by western blotting with anti-FLAG M2 antibody and anti-S-tag antibody (Novagen, Madison, WI), or antibodies for HIF-1α and HIF-2α.

Statistical Analysis

Data were expressed as mean ± standard error (S.E.). Comparisons of parameters among groups were made by one-way analysis of variance (ANOVA), followed by Newman–Keuls' test. Differences were considered significant at $P<0.05$.

Results

HIF-1α and HIF-2α Activate the CD133 Promoter

To reveal the molecular mechanisms of CD133 gene expression, we first used HEK293 cells. A reporter gene assay showed that the P5 basal activity was highest among the five putative CD133 promoters, and overexpression of HIF-1α and HIF-2α increased the activity of all promoters (Fig. 1B). In particular, P5

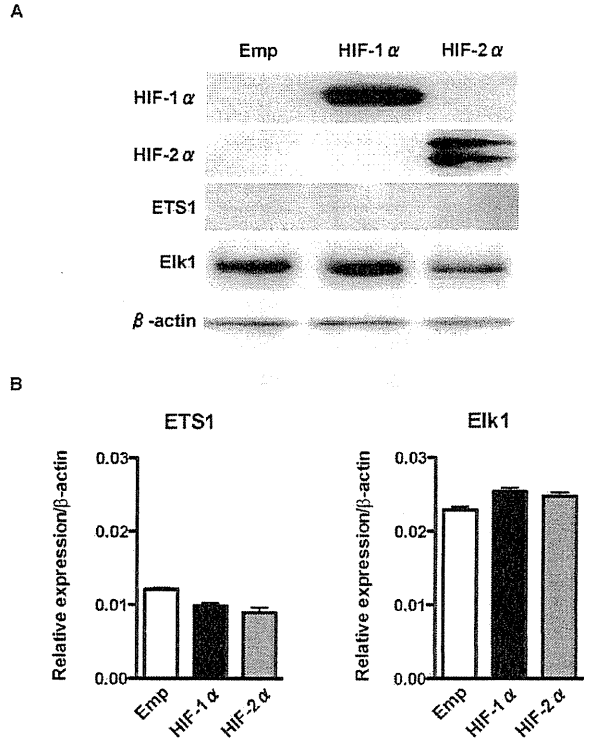

Figure 4. Effect of overexpression of HIFs on the expression of ETS-family transcription factors. (A) Western blot analysis of HIF-1α, HIF-2α, and ETS-family transcription factors after overexpression of HIF-1α or HIF-2α using human embryonic kidney (HEK) 293 cells. β-actin is an internal control. (B) Quantitavive real-time reverse-transcription PCR (qRT-PCR) of ETS-family transcription factors after overexpression of HIF-1α or HIF-2α using HEK293 cells. Data are shown as relative to the expression of β-actin.
doi:10.1371/journal.pone.0066255.g004

promoter activity was upregulated approximately 4-fold and 2.5-fold after overexpression of HIF-1α and HIF-2α, respectively. Human colon cancer WiDr cells had an effect similar to that of HEK293 cells (Fig. 1B). Although P5 promoter activity was upregulated by hypoxia, the extent of upregulation was not as enormous as with overexpression of HIF-1α or HIF-2α in HEK293 cells and WiDr cells (Fig. 1C and 1D, respectively).

The Region between −98 and −25 is Required for Upregulation of CD133 P5 Promoter Activity by HIF-1α and HIF-2α

To determine the region in the P5 promoter essential for HIF-1α- and HIF-2α-induced activation, we performed reporter gene assays using a series of P5 promoter deletion mutants of (pGL3enh-P5−768 bp, −368 bp, −98 bp, −25 bp). Without overexpression of HIF-1α or HIF-2α, deletion to −98 bp demonstrated highest activity; however, further deletion to −25 bp led to a significant reduction in activity (Fig. 2A), suggesting that the region between −98 bp and −25 bp is required for promoter activity. Upregulation of P5 activity by HIF-1α and HIF-2α was maintained until deletion to −98; however, remarkable reduction of the promoter activity was observed by further deletion to −25. HIF-1α and HIF-2α dose dependently increased the P5 −98 bp promoter activity, respectively (Fig. 2B).

EBS is Required for CD133 P5 Promoter Activity

The region between −98 bp and −25 bp of the P5 promoter contains two EBSs [21,22]. To determine whether these EBSs are required for promoter activation by HIF-1α and HIF-2α, EBS mutants (mEBS1 and mEBS2) were constructed, and a reporter gene assay was performed. The promoter activity of the proximal site mutant (mEBS2) decreased significantly under overexpression of HIF-1α or HIF-2α (Fig. 3A). To investigate the involvement of ETS-family proteins in this region, two dominant negative ETS mutants (ETS1-DN and Elk1-DN) were constructed, and the promoter activity of P5 −98 bp was analyzed. Promoter activity driven by HIF-1α and HIF-2α was decreased by ETS1-DN and Elk1-DN, respectively, suggesting that HIF-1α and HIF-2α regulate P5 −98 bp promoter activity through ETS-family proteins (Fig. 3B and 3C).

Expression of ETS-family Proteins is not Affected by Overexpression of HIF-1α and HIF-2α

Because the P5 −98 bp promoter does not contain an HRE, we hypothesized that HIF-1α and HIF-2α activate the P5 −98 bp promoter through upregulation of ETS-family proteins. However, western blotting (Fig. 4A) and qRT-PCR analysis (Fig. 4B) demonstrated that the expressions levels of ETS1 and Elk1 were not affected after HIF-1α or HIF-2α overexpression, respectively. These results suggest that HIF-1α and HIF-2α activate the P5 −98 bp promoter not by upregulation of ETS-family proteins but through other mechanisms involving ETS-family proteins.

HIF-1α Binds to the CD133 P5 Proximal Promoter through Elk1

Next we examined whether HIF-1α and HIF-2α bind to the CD133 P5 −98 bp promoter through ETS proteins in human colon cancer WiDr cells that express abundant CD133 mRNA and protein. A ChIP assay showed that FLAG-tagged O_2-stable HIF-1α or HIF-2α mutant bound to the region between −98 bp and +10 bp of the the P5 promoter, which comprises EBS2, more efficiently than to the FLAG-tagged empty vector (Fig. 5A). These results suggest that HIF-1α and HIF-2α bind to the CD133 P5 promoter through ETS proteins. We then used co-immunoprecipitation analysis to investigate whether HIF-1α and HIF-2α bind to ETS proteins in HEK293 as well as WiDr. As shown in Fig. 5B, HIF-1α bind to Elk1, but not ETS1 in both HEK293 and WiDr. However, HIF-2α did not bind to Elk1 or ETS1. Upregulation of the P5 promoter by HIF-1α was significantly suppressed by knockdown of Elk1 (Fig. 5C). Hypoxia did not influence the amount of HIF-1α and Elk1 binding (Fig. 5D).

Proximal P5 Promoter Activity and Expression of CD133 were Regulated by HIF-1α and HIF-2α in the CD133-positive Colon Cancer Cell Line WiDr

To verify the mechanisms observed in HEK293 cells, we repeated our expreriments using WiDr cells. A reporter gene assay was performed on the P5 −98 bp promoter, which showed that promoter activity was significantly decreased by knockdown of both HIF-1α and HIF-2α (Fig. 6A). Furthermore, knockdown of Elk1, but not ETS1, significantly decreased the P5 −98 bp promoter activity (Fig. 6B). Decreased activity of P5 −98 bp promoter by the knockdown of both HIF-1α and HIF-2α was recovered after overexpression of both HIF-1α and HIF-2α (Fig. 6C).

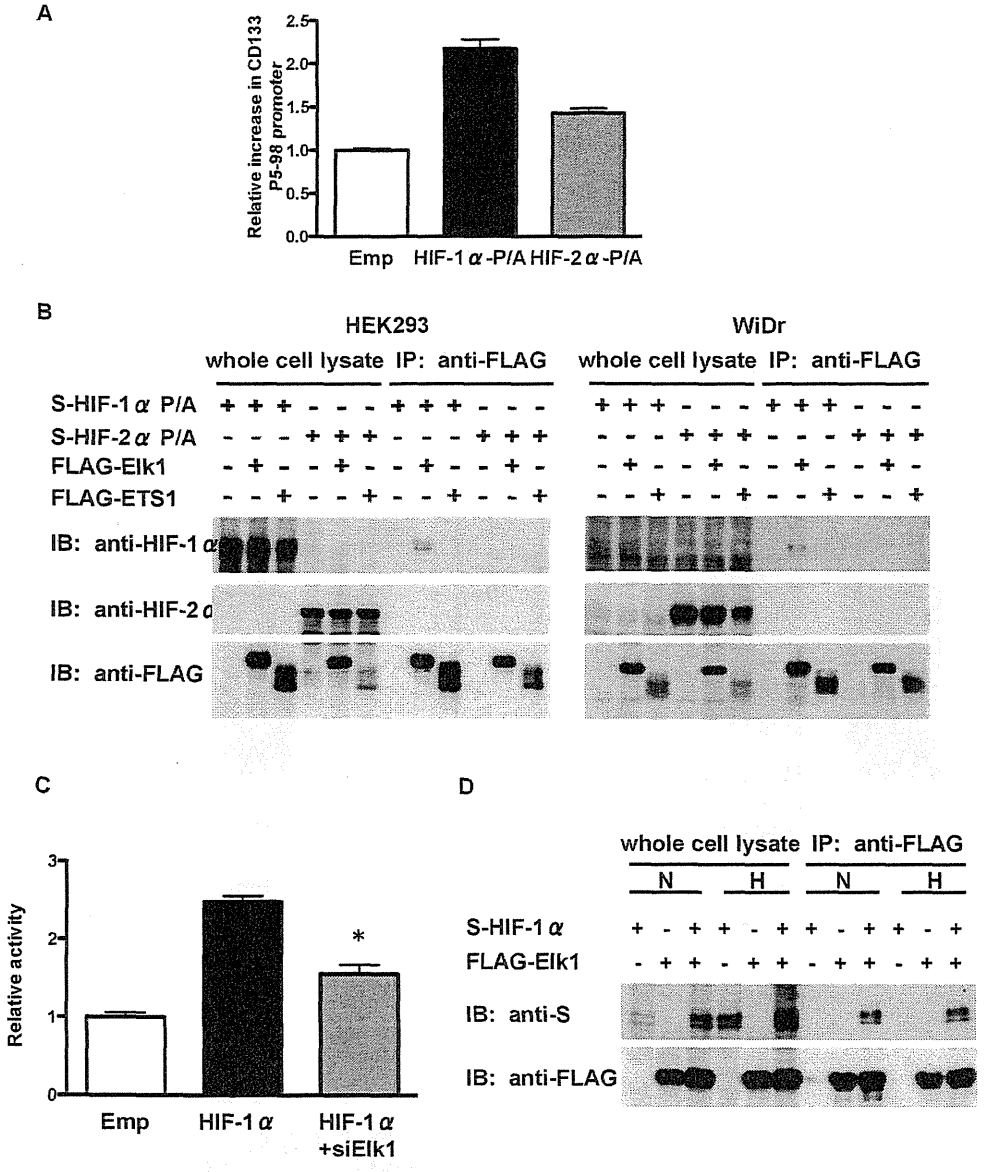

Figure 5. Binding of HIFs to CD133 P5 proximal promoter and ETS-family proteins. (A) Chromatin immunoprecipitation (ChIP) assay showing the binding of O_2-stable HIF-1α and HIF-2α (HIF-1α-P/A and HIF-2α-P/A, respectively) to the CD133 P5 promoter (between −98 bp and +10 bp) in WiDr cells. (B) IP-western blot analysis showing the binding of HIF-1α-P/A and HIF-2α-P/A to ETS1 or Elk1 using human embryonic kidney (HEK) 293 cells (left) and WiDr cells (right). (C) Luciferase activity of P5 −98 bp promoter in HEK293 cells after overexpression of HIF-1α together with the knockdown of Elk1. *$P<0.05$ vs. HIF-1α overexpression. (D) IP-western blot analysis showing the binding of HIF-1α to Elk1 under normoxia and hypoxia in HEK293 cells.
doi:10.1371/journal.pone.0066255.g005

To confirm the effect of HIF-1α and HIF-2α on CD133 transcripts and proteins, qRT-PCR and western blotting were conducted under normoxic conditions. Consistent with the results of the reporter gene assay, expression of CD133 mRNA and protein decreased when both HIF-1α and HIF-2α were knocked down (Fig. 6D and 6E, respectively).

Discussion

In this study, we focused on the regulation of CD133 by HIF-1α and HIF-2α, and demonstrated that 1) HIF-1α and HIF-2α upregulate CD133 promoter activity, particularly of P5, 2) HIF-1α and HIF-2α bind to the proximal CD133 P5 promoter at EBS, 3) HIF-1α physically interacts with Elk1, and 4) expression of CD133 is regulated by HIF-1α and HIF-2α in colon cancer cells.

Among the five alternative promoters of CD133, P1 has been reported to be most strongly associated with hypoxia-induced

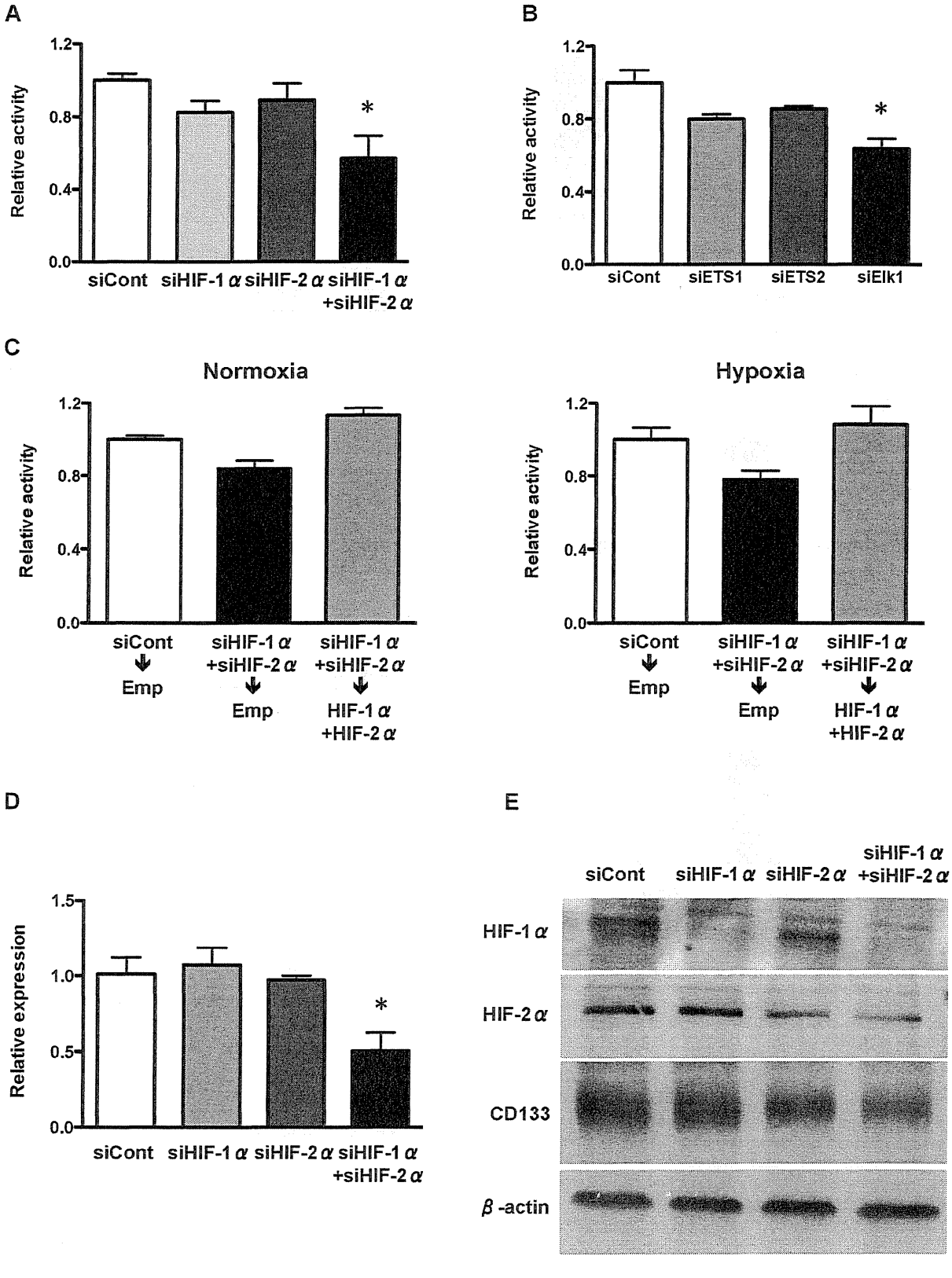
A
Relative activity
1.2
0.8
0.4
0.0
*
siCont
siHIF-1 α
siHIF-2 α
siHIF-1 α +siHIF-2 α
B
Relative activity
1.2
0.8
0.4
0.0
*
siCont
siETS1
siETS2
siElk1
C
Normoxia
Relative activity
1.2
0.8
0.4
0.0
siCont
Emp
siHIF-1 α +siHIF-2 α
Emp
siHIF-1 α +siHIF-2 α
HIF-1 α +HIF-2 α
Hypoxia
Relative activity
1.2
0.8
0.4
0.0
siCont
Emp
siHIF-1 α +siHIF-2 α
Emp
siHIF-1 α +siHIF-2 α
HIF-1 α +HIF-2 α
D
Relative expression
1.5
1.0
0.5
0.0
*
siCont
siHIF-1 α
siHIF-2 α
siHIF-1 α +siHIF-2 α
E
siCont
siHIF-1 α
siHIF-2 α
siHIF-1 α +siHIF-2 α
HIF-1 α
HIF-2 α
CD133
β -actin

Figure 6. Effect of HIFs or ETS knockdown on CD133 promoter activity and expression in WiDr cells. (A) P5 −98 bp promoter activity under knockdown of HIF-1α and HIF-2α. (B) P5 −98 bp promoter activity under knockdown of ETS families. (C) P5 −98 bp promoter activity after overexpression of HIF-1α and HIF-2α 24 hrs after knockdown of HIF-1α and HIF-2α under normoxia and hypoxia. (D) Quantitative real-time reverse-transcription PCR (qRT-PCR) analysis of CD133 under knockdown of HIF-1α and HIF-2α. *$P<0.05$ vs. control siRNA (siCont). (E) Western blot analysis of HIF-1α and HIF-2α and CD133 under knockdown of HIF-1α and HIF-2α. β-actin is an internal control.
doi:10.1371/journal.pone.0066255.g006

promoter activity and gene expression of CD133 in lung cancer cell lines [20]. In addition, Oct3/4 and Sox2, both of which are induced by HIF-1α and HIF-2α, promoted CD133 expression through their direct interaction with the P1 promoter. In contrast, our observation demonstrated that P5, but not P1, had the highest upregulation by the overexpression of HIF-1α and HIF-2α in HEK293 cells and WiDr (Fig. 1C and D). We speculate that these differences are due to the use of different cell lines, different hypoxic conditions (0.1% vs. 1%), and different P1 promoter constructs; the length of P1 promoter was rather longer than that used in this study (1800 bp vs. 1368 bp) [20]. In line with our results, it has also been reported that P5 activity was highest in the colon cancer cell line Caco-2 [21]. Therefore, we focused on the regulation of P5 promoter activity by HIF-1α and HIF-2α independent of hypoxia.

Our results suggest that HIF-1α and HIF-2α are involved in transcriptional regulation of CD133. However, P5 does not comprise an HRE, but comprises two EBSs instead.

Our results are consistent with those of a previous study in which overexpression of ETS2-DN and Elk1-DN significantly decreased the P5 promoter activity in colon cancer cells [21]. The ETS family includes nuclear phosphoproteins involved in many biological processes, such as cell growth, differentiation and survival [23]. Recently, it has been reported that HIF-1α and HIF-2α physically and functionally associate with ETS-family transcription factors. For example, ETS variant-4 (ETV4), a member of the ETS family of proteins, can activate the prolyl-4-hydroxylase domain 2 (PHD2) promoter in cooperation with HIF-1α through the HIF binding site [24], and HIF-2α activates the VE-cadherin promoter independently of hypoxia and in synergy with ETS1 through EBS [25]. In addition, glutathione S-transferase (GST) pull-down assay demonstrated that HIF-2α physically interacts with ETS1 [26], and immunoprecipitation analysis showed that HIF-2α forms a complex with Elk1 in MCF7 (breast cancer) and 786-O (renal cell carcinoma) cells [27]. Therefore, we hypothesized that HIF-1α and HIF-2α regulate CD133 promoter activity through ETS-family transcription factors. In the present study, EBS2 located in the region between −98 bp and −25 bp was found to be essential for HIF-induced activation of the P5 promoter. Additionally, a ChIP assay showed that HIF-1α and HIF-2α bind to the proximal P5 promoter harboring EBS2 and HIF-1α physically interacts with Elk1. These data strongly suggest that HIF-1α transcriptionally activates the P5 promoter through EBS2 by forming a complex with Elk1. Although we could not detect a physical interaction between HIF-2α and ETS1 or Elk1 (Fig. 5B), a ChIP assay showed that HIF-2α binds to the proximal P5 promoter harboring EBS (Fig. 5A), suggesting that HIF-2α regulates the P5 promoter through interaction with other ETS-family proteins. Further analysis is required to identify the ETS-family transcription factors that are involved in HIF-2α-meditaed activation of the P5 promoter.

Our observations suggest that HIF-1α and HIF-2α regulate CD133 transcription; however, promoter activity was not significantly upregulated by hypoxia. Unlike our findings, it has been reported that hypoxia downregulated CD133 transcription and that mTOR signaling and HIF-1α are involved in regulating CD133 expression [28]. Although the reason for this is unclear, it is possible that HIFs are regulated by other mechanisms, such as ras-mitogen-activated protein kinase (RAS-MAPK) signaling. Recently, the ras/extracellular singnal-activated kinase (RAS/ERK) signaling pathway has been demonstrated to promote CD133 transcription in colon cancer cells [21]. In addition, inhibition of the phosphatidylinositol 3-kinase (PI3K)-Akt or ERK1/2 pathway reduced the hypoxia-driven CD133 expansion in glioma cells [19]. HIF-1α can be stabilized not only through hypoxia, but also through oncogenic signaling pathways including RAS, and ERK1/2 can directly phosphorylate HIF-1α [29,30]. HIF-1α has also been shown to possess a MAPK docking domain and to bind to ERK2 [31]. Therefore, our observation could imply that the RAS/ERK signaling pathway promotes CD133 transcription through HIF-1α and HIF-2α, independently of hypoxia.

Recently, it has been demonstrated that the expression of CD133 was upregulated under hypoxia in a HIF-1α-dependent manner in pancreatic cancer cells, and knockdown of HIF-1α partially abrogated the elevated CD133 expression under hypoxia [32]. In addition, hypoxia promoted expansion of the CD133-positive glioma stem cells through activation of HIF-1α, and the CD133 expression level was increased under the chemical hypoxia in renal cancer cell lines [19,33]. Furthermore, hypoxia induced CD133 expression in human lung cancer cells by upregulation of Oct3/4 and Sox2 through HIF-1α and HIF-2α [20]. In the present study, however, hypoxia did not influence the expression of CD133 in WiDr cells (data not shown), and upregulation of P5 promoter activity under hypoxia was not as significant as with overexpression of HIF-1α or HIF-2α in HEK293 and WiDr cells (Fig. 1B-D). Furthermore, knockdown of both HIF-1α and HIF-2α under normoxia downregulated the expression of CD133 in WiDr (Fig. 6D and 6E). These results suggest that HIF1-α and HIF-2α regulate the promoter activity and expression of CD133 independently of hypoxia in colon cancer cells. In accordance to our results, it has also been demonstrated that HIF-1α enhances tumor-initiating cell frequency *in vivo* in part by regulation of the expression of CD133 and the Notch pathway in breast cancer cells [34].

Taken together, the results of the present study suggest that HIF-1α and HIF-2α regulate the expression of CD133 by controlling CD133 promoter activity, possibly through ETS proteins. Elucidating the mechanisms underlying transcriptional regulation of cancer stem cell markers such as CD133 may lead to the development of a novel target to eradicate CSC.

Acknowledgments

We thank Rika Nagashima for technical assistance.

Author Contributions

Conceived and designed the experiments: SO KN HT. Performed the experiments: SO OM AK KO HF RH KT. Analyzed the data: SO KN MA NS MK HT. Contributed reagents/materials/analysis tools: OM KN AK KO HF RH HT. Wrote the paper: SO KN HT.

References

1. Visvader JE, Lindeman GJ (2008) Cancer stem cells in solid tumours: accumulating evidence and unresolved questions. Nat Rev Cancer 8: 755–768.
2. Singh SK, Hawkins C, Clarke ID, Squire JA, Bayani J, et al. (2004) Identification of human brain tumour initiating cells. Nature 432: 396–401.
3. Collins AT, Berry PA, Hyde C, Stower MJ, Maitland NJ (2005) Prospective identification of tumorigenic prostate cancer stem cells. Cancer Res 65: 10946–10951.
4. Yin S, Li J, Hu C, Chen X, Yao M, et al. (2007) CD133 positive hepatocellular carcinoma cells possess high capacity for tumorigenicity. Int J Cancer 120: 1444–1450.
5. Hermann PC, Huber SL, Herrler T, Aicher A, Ellwart JW, et al. (2007) Distinct populations of cancer stem cells determine tumor growth and metastatic activity in human pancreatic cancer. Cell Stem Cell 1: 313–323.
6. O'Brien CA, Pollett A, Gallinger S, Dick JE (2007) A human colon cancer cell capable of initiating tumour growth in immunodeficient mice. Nature 445: 106–110.
7. Ricci-Vitiani L, Lombardi DG, Pilozzi E, Biffoni M, Todaro M, et al. (2007) Identification and expansion of human colon-cancer-initiating cells. Nature 445: 111–115.
8. Miraglia S, Godfrey W, Yin AH, Atkins K, Warnke R, et al. (1997) A novel five-transmembrane hematopoietic stem cell antigen: isolation, characterization, and molecular cloning. Blood 90: 5013–5021.
9. Yin AH, Miraglia S, Zanjani ED, Almeida-Porada G, Ogawa M, et al. (1997) AC133, a novel marker for human hematopoietic stem and progenitor cells. Blood 90: 5002–5012.
10. Shmelkov SV, Jun L, St Clair R, McGarrigle D, Derderian CA, et al. (2004) Alternative promoters regulate transcription of the gene that encodes stem cell surface protein AC133. Blood 103: 2055–2061.
11. Tabu K, Sasai K, Kimura T, Wang L, Aoyanagi E, et al. (2008) Promoter hypomethylation regulates CD133 expression in human gliomas. Cell Res 18: 1037–1046.
12. Yi JM, Tsai HC, Glöckner SC, Lin S, Ohm JE, et al. (2008) Abnormal DNA methylation of CD133 in colorectal and glioblastoma tumors. Cancer Res 68: 8094–8103.
13. Semenza GL (2003) Targeting HIF-1 for cancer therapy. Nat Rev Cancer 3: 721–732.
14. Rasheed S, Harris AL, Tekkis PP, Turley H, Silver A, et al. (2009) Hypoxia-inducible factor-1alpha and -2alpha are expressed in most rectal cancers but only hypoxia-inducible factor-1alpha is associated with prognosis. Br J Cancer 100: 1666–1673.
15. Baba Y, Nosho K, Shima K, Irahara N, Chan AT, et al. (2010) HIF1A overexpression is associated with poor prognosis in a cohort of 731 colorectal cancers. Am J Pathol 176: 2292–2301.
16. Wang GL, Jiang BH, Rue EA, Semenza GL (1995) Hypoxia-inducible factor 1 is a basic-helix-loop-helix-PAS heterodimer regulated by cellular O2 tension. Proc Natl Acad Sci U S A 92: 5510–5514.
17. Loboda A, Jozkowicz A, Dulak J (2010) HIF-1 and HIF-2 transcription factors - Similar but not identical. Mol Cells 29: 435–442.
18. Heddleston J, Li Z, Lathia J, Bao S, Hjelmeland A, et al. (2010) Hypoxia inducible factors in cancer stem cells. Br J Cancer 102: 789–795.
19. Soeda A, Park M, Lee D, Mintz A, Androutsellis-Theotokis A, et al. (2009) Hypoxia promotes expansion of the CD133-positive glioma stem cells through activation of HIF-1alpha. Oncogene 28: 3949–3959.
20. Iida H, Suzuki M, Goitsuka R, Ueno H (2012) Hypoxia induces CD133 expression in human lung cancer cells by up-regulation of OCT3/4 and SOX2. Int J Oncol 40: 71–79.
21. Tabu K, Kimura T, Sasai K, Wang L, Bizen N, et al. (2010) Analysis of an alternative human CD133 promoter reveals the implication of Ras/ERK pathway in tumor stem-like hallmarks. Mol Cancer 9: 39.
22. Fisher RJ, Mavrothalassitis G, Kondoh A, Papas TS (1991) High-affinity DNA-protein interactions of the cellular ETS1 protein: the determination of the ETS binding motif. Oncogene 6: 2249–2254.
23. Sharrocks AD (2001) The ETS-domain transcription factor family. Nat Rev Mol Cell Biol 2: 827–837.
24. Wollenick K, Hu J, Kristiansen G, Schraml P, Rehrauer H, et al. (2012) Synthetic transactivation screening reveals ETV4 as broad coactivator of hypoxia-inducible factor signaling. Nucleic Acids Res 40: 1928–1943.
25. Le Bras A, Lionneton F, Mattot V, Lelièvre E, Caetano B, et al. (2007) HIF-2alpha specifically activates the VE-cadherin promoter independently of hypoxia and in synergy with Ets-1 through two essential ETS-binding sites. Oncogene 26: 7480–7489.
26. Elvert G, Kappel A, Heidenreich R, Englmeier U, Lanz S, et al. (2003) Cooperative interaction of hypoxia-inducible factor-2alpha (HIF-2alpha) and Ets-1 in the transcriptional activation of vascular endothelial growth factor receptor-2 (Flk-1). J Biol Chem 278: 7520–7530.
27. Aprelikova O, Wood M, Tackett S, Chandramouli GV, Barrett JC (2006) Role of ETS transcription factors in the hypoxia-inducible factor-2 target gene selection. Cancer Res 66: 5641–5647.
28. Matsumoto K, Arao T, Tanaka K, Kaneda H, Kudo K, et al. (2009) mTOR signal and hypoxia-inducible factor-1 alpha regulate CD133 expression in cancer cells. Cancer Res 69: 7160–7164.
29. Harris AL (2002) Hypoxia–a key regulatory factor in tumour growth. Nat Rev Cancer 2: 38–47.
30. Mylonis I, Chachami G, Samiotaki M, Panayotou G, Paraskeva E, et al. (2006) Identification of MAPK phosphorylation sites and their role in the localization and activity of hypoxia-inducible factor-1alpha. J Biol Chem 281: 33095–33106.
31. Karapetsas A, Giannakakis A, Pavlaki M, Panayiotidis M, Sandaltzopoulos R, et al. (2011) Biochemical and molecular analysis of the interaction between ERK2 MAP kinase and hypoxia inducible factor-1α. Int J Biochem Cell Biol 43: 1582–1590.
32. Hashimoto O, Shimizu K, Semba S, Chiba S, Ku Y, et al. (2011) Hypoxia induces tumor aggressiveness and the expansion of CD133-positive cells in a hypoxia-inducible factor-1α-dependent manner in pancreatic cancer cells. Pathobiology 78: 181–192.
33. Sun C, Song H, Zhang H, Hou C, Zhai T, et al. (2012) CD133 expression in renal cell carcinoma (RCC) is correlated with nuclear hypoxia-inducing factor 1α (HIF-1α). J Cancer Res Clin Oncol.
34. Schwab LP, Peacock DL, Majumdar D, Ingels JF, Jensen LC, et al. (2012) Hypoxia-inducible factor 1α promotes primary tumor growth and tumor-initiating cell activity in breast cancer. Breast Cancer Res 14: R6.

HEPATOLOGY
Official Journal of the American Association for the Study of Liver Diseases

Wnt5a Signaling Mediates Biliary Differentiation of Fetal Hepatic Stem/Progenitor Cells in Mice

Kei Kiyohashi,[1]* Sei Kakinuma,[1,2]* Akihide Kamiya,[3,7] Naoya Sakamoto,[1,4] Sayuri Nitta,[1] Hideto Yamanaka,[1] Kouhei Yoshino,[1] Junko Fujiki,[1] Miyako Murakawa,[1] Akiko Kusano-Kitazume,[1] Hiromichi Shimizu,[1] Ryuichi Okamoto,[1] Seishin Azuma,[1] Mina Nakagawa,[1] Yasuhiro Asahina,[1,2] Naoki Tanimizu,[5] Akira Kikuchi,[6] Hiromitsu Nakauchi,[3] and Mamoru Watanabe[1]

The molecular mechanisms regulating differentiation of fetal hepatic stem/progenitor cells, called hepatoblasts, which play pivotal roles in liver development, remain obscure. Wnt signaling pathways regulate the development and differentiation of stem cells in various organs. Although a β-catenin–independent noncanonical Wnt pathway is essential for cell adhesion and polarity, the physiological functions of noncanonical Wnt pathways in liver development are unknown. Here we describe a functional role for Wnt5a, a noncanonical Wnt ligand, in the differentiation of mouse hepatoblasts. Wnt5a was expressed in mesenchymal cells and other cells of wild-type (WT) midgestational fetal liver. We analyzed fetal liver phenotypes in Wnt5a-deficient mice using a combination of histological and molecular techniques. Expression levels of Sox9 and the number of hepatocyte nuclear factor (HNF)1β^+HNF4α^- biliary precursor cells were significantly higher in Wnt5a-deficient liver relative to WT liver. In Wnt5a-deficient fetal liver, *in vivo* formation of primitive bile ductal structures was significantly enhanced relative to WT littermates. We also investigated the function of Wnt5a protein and downstream signaling molecules using a three-dimensional culture system that included primary hepatoblasts or a hepatic progenitor cell line. *In vitro* differentiation assays showed that Wnt5a retarded the formation of bile duct–like structures in hepatoblasts, leading instead to hepatic maturation of such cells. Whereas Wnt5a signaling increased steady-state levels of phosphorylated calcium/calmodulin-dependent protein kinase II (CaMKII) in fetal liver, inhibition of CaMKII activity resulted in the formation of significantly more and larger-sized bile duct–like structures *in vitro* compared with those in vehicle-supplemented controls. *Conclusion:* Wnt5a-mediated signaling in fetal hepatic stem/progenitor cells suppresses biliary differentiation. These findings also suggest that activation of CaMKII by Wnt5a signaling suppresses biliary differentiation. (HEPATOLOGY 2013;57:2502-2513)

Hepatic stem cells are multipotent stem cells located within ductal plates in fetal and neonatal livers, and canals of Hering in pediatric and adult livers.[1] The extrahepatic stem cell niches are peribiliary glands within the bile ducts in humans.[2] Hepatic stem/progenitor cells, called hepatoblasts in

Abbreviations: Ab, antibody; AFP, α-fetoprotein; ALB, albumin; CaMKII, calcium/calmodulin-dependent kinase II; CK, cytokeratin; CPS1, carbamoyl phosphate synthetase 1; DAPI; 4',6-diamidino-2-phenylindole; DMEM, Dulbecco's modified Eagle's medium; DMSO, dimethyl sulfoxide; E, embryonic day; EHS, Engelbreth-Holm-Swarm; FCS, fetal calf serum; Fzd, Frizzled; G6Pase, glucose 6-phosphatase; HGF, hepatocyte growth factor; HNF, hepatocyte nuclear factor; KO, knockout; mRNA, messenger RNA; MRP3, multidrug resistance–associated protein 3; NLK, Nemo-like kinase; P, postnatal day; PCNA, proliferating cell nuclear antigen; PDS, primitive ductal structure; PKC, protein kinase C; RT-PCR, reverse-transcriptase polymerase chain reaction; TAK1, transforming growth factor β–activated kinase 1; WT, wild-type.

From the Department of [1]Gastroenterology and Hepatology and [2]Department for Hepatitis Control, Tokyo Medical and Dental University, Tokyo, Japan; the [3]Division of Stem Cell Therapy, Institute of Medical Science, The University of Tokyo, Tokyo, Japan; the [4]Department of Gastroenterology and Hepatology, Hokkaido University, Sapporo, Japan; the [5]Department of Tissue Development and Regeneration, School of Medicine, Sapporo Medical University, Sapporo, Japan; the [6]Department of Molecular Biology and Biochemistry, Graduate School of Medicine, Osaka University, Osaka, Japan; and the [7]Institute of Innovative Science and Technology, Tokai University, Isehara, Japan.

Received May 11, 2012; accepted January 7, 2013.

This work was supported in part by Grants-in-Aid for Scientific Research from the Ministry of Education, Culture, Sports, Science and Technology in Japan; the Ministry of Health, Labor and Welfare in Japan; the Japan Society for the Promotion of Science, the Japan Health Sciences Foundation; the National Institute of Biomedical Innovation; and the Foundation for Advancement of International Science.

**These authors contributed equally to this work.*

the fetal liver, proliferate actively and give rise to hepatocytes and cholangiocytes.[3,4] Lineage commitment of such cells can be traced by several cell surface markers, including NCAM, ICAM-1, and EpCAM in humans.[1,5] While our group[6] and others[7] demonstrated roles for transcription factors regulating the biliary differentiation of hepatic stem/progenitor cells, the molecular mechanisms behind these events have yet to be fully elucidated.

The Wnt family secreted ligands and the corresponding Frizzled family cell surface receptors play a crucial role in the differentiation, proliferation, and self-renewal of stem cells in various organs.[8] Wnt signaling pathways involve interactions between a complex set of molecular cognates that includes 19 different Wnt ligands and 10 Frizzled (Fzd) receptors in humans and mice (reviewed at http://www.stanford.edu/group/nusselab/cgi-bin/wnt/). Upon binding to Fzd receptors on the surface of a target cell, Wnt proteins activate one of two classes of downstream pathways distinguishable by their dependency on β-catenin. Examples of canonical β-catenin–dependent pathways include β-catenin–dependent activation of T cell factor by either Wnt1 or Wnt3.[8] In contrast, Wnt4 and Wnt5a activate noncanonical β-catenin–independent pathways that include downstream molecules such as calcium/calmodulin-dependent protein kinase II (CaMKII), Rho-kinase, Rac1, calcineurin, and protein kinase C (PKC).[9]

In liver development, β-catenin is known to regulate the maturation, expansion, and survival of hepatoblasts, and its deletion results in increased apoptosis of hepatoblasts in midgestational fetal livers.[10] While the function of noncanonical Wnt signaling in liver development is currently unknown, β-catenin–independent Wnt pathways have been shown to function predominantly as regulators of cell polarity and mobility in other organs.[9] In systemic Wnt5a-deficient (knockout [KO]) mice, the size of caudal structures, lung morphogenesis, and intestinal elongation are also abnormal.[11–13]

Recent reports demonstrate that Wnt5a regulates hematopoietic, mesenchymal, and neural stem cell functions.[14-16] Wnt5a has been shown to increase the repopulation of short- and long-term hematopoietic stem cells by maintaining these cells in a quiescent G0 state.[14] Wnt5a maintains mesenchymal stem cells and promotes osteoblastogenesis in preference to adipogenesis in bone marrow,[15] and also improves the differentiation and functional integration of stem cell–derived dopamine neurons.[16] In healthy adult mouse liver, Wnt5a is expressed in mature hepatocytes and cholangiocytes.[17] Nonetheless, the physiological functions of Wnt5a and the signaling cascades that it initiates during liver development and in hepatic stem/progenitor cells are unknown.

In this study, we investigated the function of Wnt5a and its downstream targets in the development of murine fetal hepatic stem/progenitor cells. Analysis of Wnt5a KO mice demonstrated that loss of Wnt5a abnormally promotes the formation of bile ductal structures in fetal liver *in vivo*. Wnt5a supplementation not only retarded the formation of bile duct–like structures, but also promoted hepatic maturation of hepatic stem/progenitor cells *in vitro*. CaMKII activity, which showed Wnt5a dependence in fetal liver, suppressed the formation of bile duct–like structures. These data indicate that Wnt5a-mediated CaMKII signaling plays an essential role in the differentiation of murine fetal hepatic stem/progenitor cells.

Materials and Methods

Animals. Systemic Wnt5a KO mice in C57BL/6 background were originally generated by Yamaguchi et al.[11] Wnt5a KO mice and wild-type (WT) littermates were produced by crossbreeding Wnt5a heterozygous mice. All animals were treated based on the guidelines of the Institute of Medical Science, University of Tokyo, and those of Tokyo Medical and Dental University.

In Vitro *Bile Duct–Like Differentiation Assay of Primary Hepatoblasts.* Bile duct–like differentiation assays were performed as described[6] with some modifications. Fetal hepatic cells of embryonic day (E) 14.5 liver were dissociated with collagenase,[4] and Dlk^+ cells were isolated from the resulting population using a magnetic cell sorter (Miltenyi Biotec, Bergisch Gladbach, Germany) and then cultured in collagen gel

Address reprint requests to: Sei Kakinuma, M.D., Ph.D., and Mamoru Watanabe, M.D., Ph.D., Department of Gastroenterology and Hepatology, Tokyo Medical and Dental University, 1-5-45 Yushima, Bunkyo-ku, Tokyo, 1138519 Japan. E-mail: skakinuma.gast@tmd.ac.jp (S. K.) and mamoru.gast@tmd.ac.jp (M. W.); fax: (81)-3-5803-0268.

View this article online at wileyonlinelibrary.com.
DOI 10.1002/hep.26293
Potential conflict of interest: Nothing to report.
Additional Supporting Information may be found in the online version of this article.